

STRUCTURAL PROPERTIES OF CROSS LAMINATED TIMBER UNDER ELEVATED
TEMPERATURE DUE TO FIRE

by

Bryce DeShazer

A thesis submitted to the Faculty and the Board of Trustees of the Colorado School of Mines in partial fulfillment of the requirements for the degree of Master of Science (Civil and Environmental Engineering)

Golden, Colorado

Date _____

Signed: _____

Bryce DeShazer

Signed: _____

Dr. Shiling Pei
Thesis Advisor

Golden, Colorado

Date _____

Signed: _____

Dr. Terri Hogue
Professor and Department Head
Civil and Environmental Engineering

ABSTRACT

At the time of this thesis work, one of the fastest growing materials in timber construction is Cross Laminated Timber (CLT). This building material has many appeals, from sustainability of production to visual aesthetics, and offers a multitude of benefits in design and construction. However, there are still areas of the design that need more research in order to better understand CLT as an engineered wood structural material in order to design safer as well as boost public trust of the material. In particular, the material behavior at elevated temperatures due to fire has a limited amount of research. This study aims to fill in the gaps in terms of material behavior of CLT as a one-way slab is heated uniformly along the bottom of its span. Through the use of computer aided finite element modeling, the stresses and deformation of CLT can be better understood and the overall impact of high temperature to beam strength, stiffness, and over-all deflection can be studied in a quantitative fashion. The simulation study for a total of 12 different wood and glue combinations in order to determine the behavior of CLT with different manufacturing material options. The small-scale experimental data from an earlier FPL study is used to obtain the material properties of wood and glue as a function of temperature. The temperature distribution along the thickness of CLT was modeled based on experimental testing data from CLT panel burning tests. The overall findings of this study suggest that the material properties behave in a linear fashion as the temperature increases. The reduction of panel stiffness and strength is very limited before charring of the wood (under 10% for most of the cases simulated). The wood materials are most likely to reach its strength limit before the glue, due to the protection of the wood and the buried glue lines. However, this study does not

consider the fire condition where wood is charred and loses all its strength. The results of this study still need to be validated using full-scale panel heating tests.

TABLE OF CONTENTS

ABSTRACT	iii
LIST OF FIGURES	vii
LIST OF TABLES.....	ix
ACKNOWLEDGEMENTS	x
CHAPTER ONE: BACKGROUND & INTRODUCTION	1
1.1 Motivation and Background	1
1.2 Extended Literature Review	3
1.3 Goal of Research.....	6
CHAPTER TWO: SMALL SPECIMEN TESTING.....	7
2.1 Background of Research	7
2.2 Small Scale Wood and Glue Tests.....	7
2.3 Test Results Implementation	11
CHAPTER THREE: RESEARCH METHODOLOGY	17
3.1 Overview of Modeling Method	17
3.2 Matlab Pre - Processing.....	19
3.3 Finite Element Modeling.....	26
3.4 Post-Processing.....	29

3.5 Model Validation	34
3.5.1 Solid Wood Beam Bending	34
3.5.1 Determination of FEM Mesh size	36
3.5.3 Layered beam with very weak coupling.....	37
CHAPTER FOUR: CLT PERFORMANCE UNDER ELEVATED TEMPERATURE	41
4.1 Methodology.....	41
4.2 Verification of Methodology	44
4.3 Effects of Temperature on Panel Properties.....	45
4.4.1 Effects with Varying Plys.....	50
4.4.2 comparisson between 3, 5, and 7 ply CLT	53
4.5 Tested temperature profile compared to potential temperature profile.....	59
CHAPTER FIVE: CONCLUSION	68
REFERENCES.....	70

LIST OF FIGURES

Figure 1.1	Typical CLT Panel Lay-Up [1].....	1
Figure 2.1	Small-Scale Testing Specimens (Wood and Glue).....	8
Figure 2.2	Average Values from Small-Scale Wood Species Tests [8]	9
Figure 2.3	Representative Shear Stress and Strain Plots for Small-Scale Glue Tests [8]	10
Figure 3.1	CLT Panel Parameters.....	20
Figure 3.2	Temperature Profile Taken from FPL Experimental Data.....	23
Figure 3.3	Material Map of CLT Panel Slab.....	28
Figure 3.4	Matlab Post-Processing Menu's	33
Figure 3.5	Deflection of Beam with Weak Coupling.....	39
Figure 3.6	Enhanced View of Beam's End with Weak Coupling.....	39
Figure 3.7	Shear Strain of Beam with Weak Coupling	40
Figure 4.1	Comparison of Room Temperature Panel and Fully Burned Panel.....	44
Figure 4.1	Deflection Curves of Varying Wood and Glue Combinations.....	46
Figure 4.2	Panel Deflection of 5 and 7 Ply Panels	51
Figure 4.3	Internal Stress in X Direction for 300°C 3-Ply Model.....	55
Figure 4.4	Internal Stress in X Direction for 300°C 5-Ply Model.....	56
Figure 4.5	Internal Stress in X Direction for 300°C 7-Ply Model.....	56
Figure 4.6	Shear Stress for 7-Ply Model at 300°C Temperature.....	58

Figure 4.7	Shear Strain for 7-Ply Model at 300°C Temperature.....	59
Figure 4.8	Theoretical Temperature Profile.....	60
Figure 4.9	Extent of Fire Impact Using Theoretical Temperature Profile.....	62
Figure 4.10	Internal Stress in X Direction for 300°C 3-Ply Model with Theoretical Profile.....	66
Figure 4.11	Internal Stress in X Direction for 300°C 5-Ply Model with Theoretical Profile.....	66
Figure 4.12	Internal Stress in X Direction for 300°C 7-Ply Model with Theoretical Profile.....	67

LIST OF TABLES

Table 2.1	Small-Scale Test Results of Wood Species	12
Table 2.2	Small-Scale Test Results of Glue Types.	12
Table 3.1	Constant Material Values	22
Table 3.2	Summary of FEM Mesh Size Tests.....	36
Table 4.2	First Stage CLT Testing Matrix.....	43
Table 4.3	Stress Limit Target Load and Limiting Material at Specified Temperatures.....	47
Table 4.4	Reduction in Stress Limit Target Load at Varying Panel Temperatures	47
Table 4.5	Deflection Stiffness of Panel at Specified Temperatures.....	49
Table 4.6	Visual Categorization of Panel Deflection Stiffness Compared to Temperature	49
Table 4.7	Second Stage CLT Testing Matrix.....	50
Table 4.8	Limit Stress Target Load and Material of Multi-Ply Combinations.....	52
Table 4.9	Reduction in Limit Stress Target Loads for Multi-Ply Combinations.....	52
Table 4.10	Panel Stiffness Trends for Varying Wood/Glue Combinations.....	53
Table 4.11	Comparison of Trends Between Varying Ply Count.....	54
Table 4.12	Testing Matrix for Theoretical Temperature Profile.....	63
Table 4.13	Limiting Stress and Material for Theoretical Temperature Profile.....	63
Table 4.14	Reduction of Limit Stress Target Load Under Theoretical Temperature Profile.....	64
Table 4.15	Deflection Stiffness of Panel Models Under Theoretical Temperature Profile.....	65

ACKNOWLEDGEMENTS

First and foremost, I would like to thank the organization that made this study possible. The funding for this research is provided by the U.S. Endowment for Forestry and Communities. Without the help of which I would not have been able to complete this study.

I would also like to acknowledge the help and data provided by the U.S. Department of Agriculture Forest Products Laboratory. The data provided was a large part of the research process presented here. However, the findings from this study are of our own, and do not reflect the opinion of the sponsor.

Additionally, I would like to thank my advisor, Dr. Shiling Pei, for the fantastic opportunity to work in this field of research. His enthusiasm, patience, and constant advice are a large part of what got me through the research portion. Through our meetings, I learned a great amount not only about timber engineering, but about general mechanics as well. Having had this experience I can confidentially say that I am entering the world as a better engineer and problem solver.

I would like to thank both of my committee members as well, Dr. Joseph Crocker, and Dr. Hongyan Liu. Both of whom have played large roles in my educational career at CSM. Having them be committee members was a humbling experience and I am looking forward to the career I can build with the tools they have given me.

Finally, I would like to thank my friends and family for remaining a constant for me throughout the process. Their interest, advice, and unconditional support were instrumental in achieving my goal.

CHAPTER ONE: BACKGROUND & INTRODUCTION

1.1 Motivation and Background

Cross Laminated Timber (CLT) as a new engineered wood structural material has been rising in popularity in recent years. First invented in Europe, a number of design codes and standards have started accepting CLT in North America, including the National Design Specification for Wood Construction (NDS) and APA PRG320, standard for performance-rated cross laminated timber. The overall concept is straightforward, layers of timber are laminated together as illustrated in Figure 1.1 in order to create large structural panels that can be used in a variety of applications. The sustainability, constructability, and architectural aesthetics of CLT are some of the major attractions for designers and owners despite its higher cost compared to traditional materials. Despite the increase in CLT usage recently, there are still areas of design that have not been thoroughly investigated due to lack of test data. One of these areas is the impact of fire on cross laminated timber panels as floor diaphragms in building.

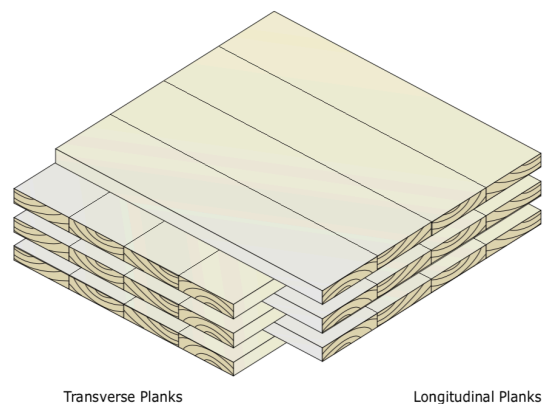


Figure 1.1 Typical CLT Panel Lay-Up [1]

Wood construction in the United States addresses fire through design using different strategies. To begin with, light frame wood buildings gain fire resistance through non-combustible gypsum board protection. Using gypsum board, a wood shear wall or floor element can gain one hour of fire rating, which allows such buildings to be built to a height of up to 85 ft. In cases with CLT and other mass timber elements (e.g. glulam beams and columns), the surface portion of the mass timber element will char during fire and will protect the inner part of the wood members. If enough sacrificial layers are added to the thickness during design, the exposed CLT can withstand extended periods of burning without failing. To develop this type of sacrificial layer in design, recommended charring rates for wood can be found in design codes and guides. The International Building Code (IBC) provides the required fire rating for different building components given the building category. Alternatively, CLT panels (as well as other mass timber members) can be protected using gypsum board. The code change proposal to IBC2021 includes tall mass timber building categories up to 18 stories tall, while requiring non-combustible protection on all wood components. While having wood covered up is not preferable to the owner and architect, one can reduce the height to 12 stories or below to be able to expose parts of the wood.

Nonetheless, for the design of CLT buildings, it is necessary to understand how the CLT panel material behaves while burning or being heated. Under normal temperatures, it is commonly understood the strength of the wood glue is higher than the wood itself. However, little is known how this statement will change as the wood and glue are heated up. There have been some CLT burning tests that revealed CLT delamination during exposed fire contact. Although the delamination does not occur until the exposed layer of CLT is charred, the extent of how much the panel is weakened by elevated temperatures is unknown. Nor are the changes

to the overall properties of CLT panels, such as strength and stiffness, known or validated through testing. This study is a follow up to another investigation on small-scale sample testing of wood and glue materials conducted at the Forest Products Laboratory (included in Chapter Two). This thesis utilizes the small-scale specimen test data to construct finite element models to assess CLT panel performance under elevated temperature.

1.2 Extended Literature Review

In the field of CLT and investigations into the material properties as a whole, a significant amount of research and effort has been put into further understanding the material behavior. The majority of effort has been directed towards understanding the interactions of the different layers, depending on the interface between them, while a handful of other studies have explored different ways that fire can impact a CLT slab panel. Quite a few relevant papers were found during the literature review portion of this study and are summarized as follows. A few are relevant to this study in terms of understanding the material behavior of the beam as a whole, while others are useful and relevant in terms of their fire applications.

The first paper considered was written concerning a composite beam element, with layer wise plane sections. The work done in this paper is built around the classical Bernoulli-Euler and Timoshenko beam theories, which were used to develop a one-dimensional laminated beam finite element with layer wise constant shear (BLCS) formulation [2]. Ultimately, the assumption of this formulation is that a first-order shear deformation occurs on each individual layer, following Timoshenko beam theory [2]. This meaning that at a given cross-section of a beam, the elements do not necessarily remain plane when crossing the laminates but remain plane only in each layer of the beam. By using this formulation, the beam is expressed as a simple beam element, with transformed layerwise shear stresses being the end results. Based on

this work, a better understanding of the plane behavior of the layers can be taken. This contributes to the assumptions of how the layers will behave at different strengths of the interlayer material. Ultimately, this paper is used in this study as verifications for how the computer models generates and analyses a layered beam.

Similar to the previous paper, the next considered was written addressing an analytical solution of two-layer beams, accounting for nonlinear interlayer slip [3]. The goal of this paper was developing an analytical (exact) model to analyze composite beams under transverse bending loading. In the case of this study, the interface layers and shear connectors are presented as elastoplastic strain-softening elements. The model developed from this predicts the stresses due to a given load and ultimate load for when debonding will occur for bi-layered composite beams. The ultimate findings from this work are the relationships between geometric and material properties and the dependence of load-carrying capacity, stresses and deflections of a local non-linear relationship. It also proves that the shear connections lower and upper bounds do not imply a lower or upper bound on the results [3]. The results from this study are useful as well given the discuss the impact on the geometric and material properties on the overall beam reactions, which is part of what this study seeks to do. However, it is only modeled on a two-layer composite beam, meaning the results cannot realistically be assumed to apply to the models developed in this study. Another paper worth mentioning is written about the analytical solution of two-layer beams, considering interlayer slip as well as shear deformation [4]. The findings of this paper are consistent with the work done in [3], with the biggest conclusion being that the effects of shear deformations are highly significant and must be addressed in design.

These three papers are all very useful in creating and understanding the computer aided model that this study uses. However, there are still other papers that utilize fire in their work. A

significant paper is written on fire tests of loaded CLT wall and floor elements. This paper mainly focused on both the impact of the cross-sectional lay up as well as different anchor types on the wall elements. The tests were run on a total of 10 differently loaded panels. The results from this study mainly focus on the charring rate of CLT under fire, which is useful to understanding CLT better in design [5]. However, this study is conducted on Canadian CLT panels, and addresses the charring rate of CLT, both of which are not included in the scope of this study.

Similarly, another paper focuses on the overall fire behavior of cross laminated solid timber panels. The goal of this study was to compare analytical and experimental results of the charring rate of CLT compared to homogenous wood. The conclusion drawn was the charring rate of CLT is consistent with the charring rate of regular wood. Additionally, it was found that vertical structural members perform better in fire than horizontal structural members [6]. While these findings are also useful in terms of fire design, this study is conducted on European CLT models, which is not entirely beneficial to design with American CLT.

The final paper considered for this study discussed the structural response of fire-exposed cross-laminated timber under sustained loads. This study focused directly on the heating of exposed CLT under sustained loads. The findings were that no significant delamination's were observed until later in the burning of the sample. Furthermore, the conclusion was that a new approach must be developed to calculate the thermo-mechanical response of CLT [7]. This paper is a good stepping stone for the goal of this thesis, as it is a small-scale test of what this study seeks to achieve. The exposed length of the CLT element in this paper is no more than 3ft, which is useful to understand CLT behavior, however it is nowhere close to a practical span of CLT in real life applications.

These papers provide a lot of insight as to the way multi-layered beams behave due to the interface layer. While there has been a decent amount of work relating to the mechanics of CLT under fire, very few papers consider full span tests of CLT under elevated temperature and quantitatively characterize their structural performance. This highlights that in terms of research, this is an area that needs more data in order to draw full conclusions as to the behavior of CLT. That is ultimately what this study seeks to achieve.

1.3 Goal of Research

The goal of this research is to further contribute to the knowledge and understanding of CLT material performance under elevated temperature. A better understanding of the behavior of CLT at elevated temperatures will contribute greatly to the public acceptance and usage of CLT. The CLT material can be used as walls and floors. In this study, we will focus on CLT applied as a one-way slab. General structural properties of a slab will be evaluated at different temperatures, these being the beams deflection, stiffness, maximum stress, and maximum strain (and estimates on strength). Failure of the panel under bending will be evaluated, as well as the mode of failure, i.e. if the wood fails first or the glue fails first. Based on the analysis, the strongest combinations of wood and glue can be determined, and the impact of temperature on different CLT combinations will be evaluated to assist CLT applications and design.

CHAPTER TWO: SMALL SPECIMEN TESTING

2.1 Background of Research

In order to understand the mechanical behavior of CLT under high temperatures, the material properties of wood and glue joints under different temperature levels must be known. While the test work was not conducted within the scope of this thesis, this study was built off of a previous study conducted at the Forest Products Lab in Madison, WI. In particular, the previous study was focused on small scale material tests on wood and glue joint strength and stiffness under different temperature levels. Brief details about this previous study are included here for convenience and understanding of the readers. The work to reorganize the test data into a format that can be used for finite element modeling was part of this study and is presented in section 2.3. This was run for three different wood species (Douglas Fir, Southern Pine, and Spruce Pine) as well as four different glue types (PUR1, PUR2, PRF, and MF). Those are very commonly used wood and glue types for CLT manufacturing in North America. Testing the range of materials contributes better to the overall understanding of delamination at elevated temperatures. Specifically, the finite element models developed in this thesis used the mechanical properties obtained through the small-scale tests.

2.2 Small Scale Wood and Glue Tests

In order to get the desired strength/stiffness values, the test program employed two different setups for the wood and glue joint. Both test setups included a uniaxial tensile machine that records the load and deflection. In order to maintain constant temperatures, the specimens were placed in an oven designed to maintain a certain temperature. The wood was tested under pure tension, while the glue was tested in shear using a half-lap joint detail. This mimics the way

the glue lines are present in CLT, which mostly was intended to transfer the shear between wood layers. The test setup and specimens are shown in Figure 2.1.

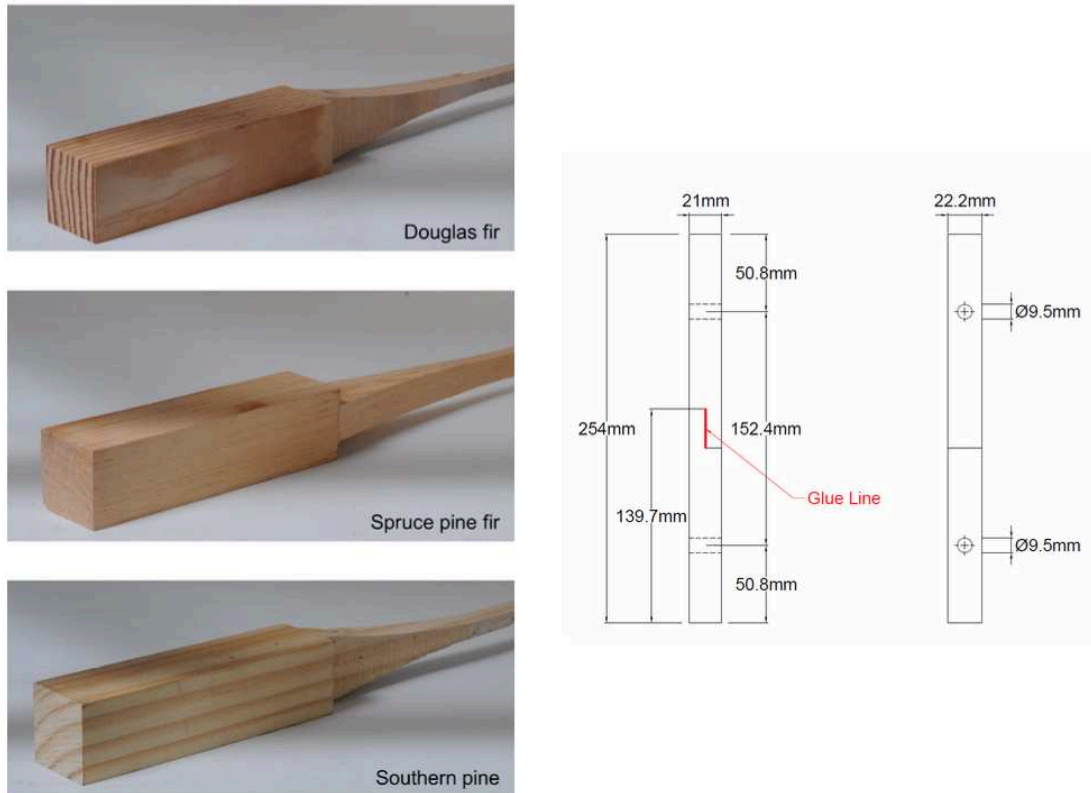


Figure 2.1 Small-Scale Testing Specimens (Wood and Glue) [8]

There was a total of three different wood species tested at five different temperature levels. Ten nominally identical specimens were constructed and tested for each wood type/temperature combination in order to obtain statistical characteristics of the test. A special oven was used to keep consistency on the temperatures, the wood was tested at the following temperatures: 25°C, 100°C, 140°C, 180°C, and 220°C. More detailed descriptions of the tests conducted, and the results can be found in [8]. Figure 2.2 shows the test results for the wood specimens.

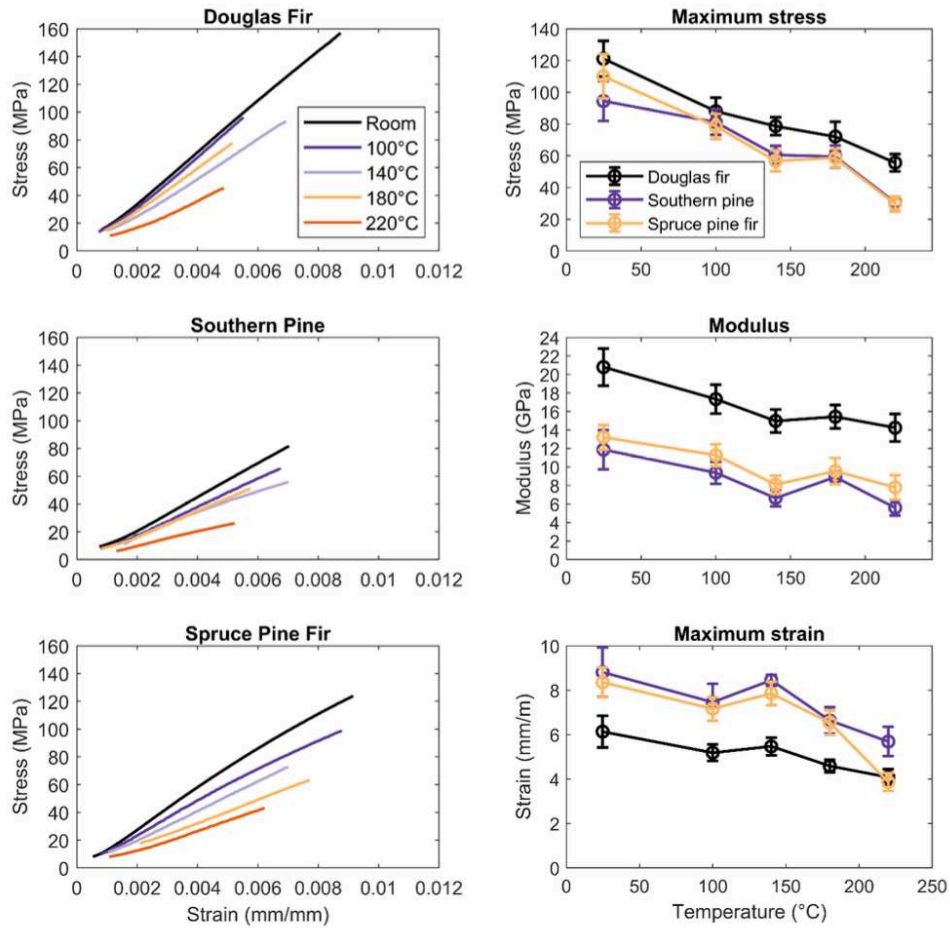


Figure 2.2 Average Values from Small-Scale Wood Species Tests [8]

In order to test the glue joint under pure shear conditions, it was constructed into a tensile specimen with a half lap joint. Due to the limited time and manpower in the small-scale testing project, the four glue types were all tested using Douglas Fir as the wood species (i.e. other wood-glue combinations were not tested). The glue test was also conducted with ten specimen repetitions at each glue-temperature combination. To ensure equality and consistency with typical CLT manufacturing process, the samples were all glued within a 3-hour window from when the lap joint was cut. The glue was not tested at room temperature because it is known that it is stronger than wood material by design. The elevated cases included the following

temperatures: 100°C, 140°C, 180°C, 220°C, and 240°C. To further enhance the study's results, each specimen was tested along with a sample of solid wood cut to mimic the half-lap connection shape, in order to normalize the temperature curve for the solid wood it was tested on. The goal of this normalization being that the material results of the glue types are adjusted to a range reflective of real-world applications. Figure 2.3 shows the results from the shear tests on the glue.

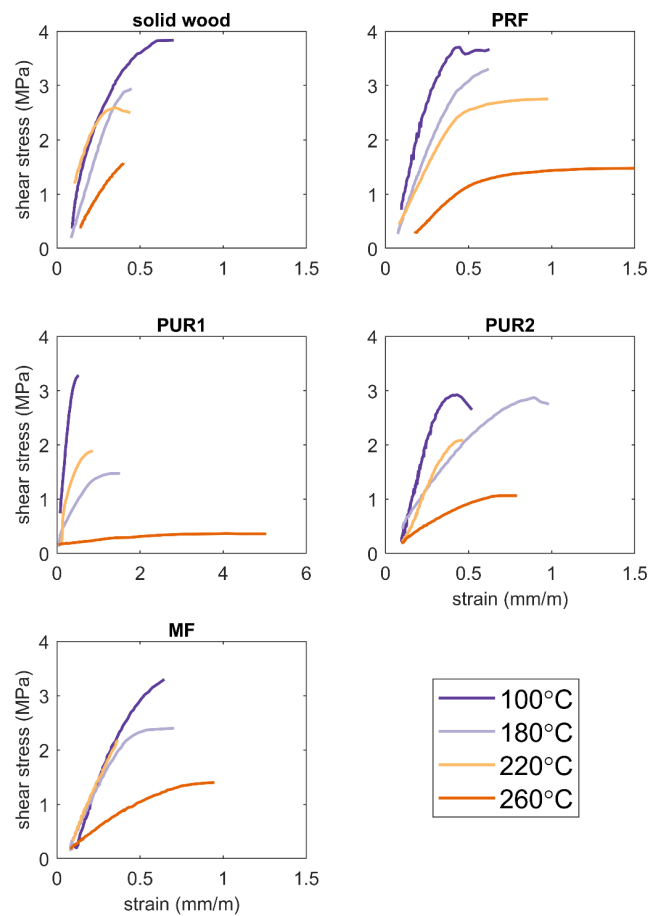


Figure 2.3 Representative Shear Stress and Strain Plots for Small-Scale Glue Tests [8]

Over all, the test results for both the wood and glue samples was qualitatively consistent with the common expectations. Overall, the maximum stress, modulus, and strain at failure for the wood species decreased as the temperature increases. The same can be stated for the glue types tested, all of which exhibited a decrease in strength/stiffness as the temperature was increased. Additionally, it is important to note that the most significant decrease in strength started at 260°C for the various glue types. The results from these small-scale tests are utilized in this thesis to model the regression of material properties vs temperature.

2.3 Test Results Implementation

In order to model the CLT panel under different temperature conditions, the results from the small-scale tests were reorganized in a format easy to use for finite element models. In order to accomplish this, stiffness and strength of the wood material and glue were calculated from the small-scale test data. The following tests list the actual stress and strain data extracted from the average results of the small-scale tests. Table 2.1 displays the resultant test values from the small-scale wood species testing, while Table 2.2 displays the resultant test values from the glue type testing.

One unique characteristic of the Mechanical properties of wood material is the size effect. Essentially, this means that the strength and stiffness measured from a small clear wood specimen (with little to no defects) will be much higher than that of larger sized wood due to the material imperfections by volume. The same can be said for glue joints, as the larger the glue area, the more likely there will be gaps and imperfections. Because of this, the measured strength and stiffness values could not be used directly for large panel modeling. Instead, we can assume that the relative level of reduction in strength and stiffness reflected in small scale testing will be similar to that in large specimens. While this assumption provides a basis of

understanding for this study, investigations into larger test specimens are required in order to validate this assumption. Thus, in this study, the strength and stiffness results at room temperature were used to normalize the test values at high temperatures and applied the relative reduction to the large panel models. The normalized strength and stiffness values (based on NDS allowable stress) are also listed in Table 2.1. While the NDS provides no basis for normalizing glue joint strength, these test values were used directly (without normalization) as they are not that far from wood strength identified in the NDS.

Table 2.1 Small-Scale Test Results of Wood Species

Maximum Tensile Stress			Room Temp (25 °C)			Max Temp (220 °C)		
	Wood Type	Stress (MPa)	Stress (psi)	Normalized Stress (psi)	Stress (MPa)	Stress (psi)	Normalized Stress (psi)	Normalized Slope (psi/°C)
	Doug Fir	125	18129.8	1500	55	7977.09	660.00	-4.31
	South Pine	110	15954.2	2350	35	5076.33	747.73	-8.22
Spruce Pine	95	13778.6	1250	35	5076.33	460.53	-4.05	

Elastic Modulus			Room Temp (25 °C)		Max Temp (220 °C)		Slope (psi/°C)
	Wood Type	E (GPa)	E (psi)	E (GPa)	E (psi)		
	Doug Fir	21	3045798	16	2320608	-3719	
	South Pine	12	1740456	5	725190	-5206	
Spruce Pine	13	1885494	8	1160304	-3719		

Table 2.2 Small-Scale Test Results of Glue Types

Maximum Shear Strength			Initial Temperature (100 °C)		Maximum Temperature (260 °C)			
	Glue Type	Max Strength (MPa)	Max Strength (psi)	Min Strength (MPa)	Min Strength (psi)	Slope (psi/°C)	Strength at 25°C	
	PUR1	3.2	464.1216	0.4	58.0152	-2.54	654.5	
	PUR2	3	435.114	1.1	159.5418	-1.72	564.3	
	PRF	3.8	551.1444	1.5	217.557	-2.08	707.5	
MF	3.5	507.633	1.4	203.0532	-1.90	650.4		

Modulus of Elasticity			Initial Temperature (100 °C)				Maximum Temperature (260 °C)			
	Glue Type	G (MPa)	Strain (mm/m)	G (psi)	E (psi)	G (MPa)	Strain (mm/m)	G (psi)	E (psi)	Slope (psi/°C)
	PUR1	3	0.3	1450380	3741980	0.2	2	14503.8	37420	-23154
	PUR2	2.5	0.3	1208650	3118317	0.9	0.5	261068.4	673556	-15280
	PRF	3	0.3	1450380	3741980	0.8	0.4	290076	748396	-18710
MF	2	0.3	966920	2494654	1	0.5	290076	748396	-10914	

The most prominent reason for assuming a linear regression in the strength and stiffness vs temperature is because a linear line was the most reasonable and simple for every case. It also simplifies the programming aspect of the FEM model generation (discussed later in Chapter 3), as well as simplifies the normalization process. To normalize the linear values, a few different approaches were used. The experimental data for the modulus of the wood samples were relatively close to the NDS values for the given wood species. The largest difference being in the Douglas fir whose experimental E was roughly 3,000,000 psi, as compared to the NDS value of 1,900,000 psi. While the error is nearly %60 percent, this difference in values can be attributed to the clear wood specimen and the embedded reliability and redundancy in the NDS values. Likewise, this can be said for the other wood species. Thus, the equations were developed using the NDS values for E, and the slopes determined from the small-scale testing. As for the maximum strength of the wood versus temperature, the similar error can be seen. Again, comparing the values of Douglas Fir, the experimental maximum strength was roughly 18000 psi, compared to the NDS value of 1500 psi. The small-scale value is over a magnitude of 10 times larger than the accepted literary value. This is likely due to the clear wood cross sections having little to no imperfection in their cross sections. To normalize the data against this, a reduction factor was determined by taking the max or min strength divided by the max strength, which was then multiplied by the NDS strength value. Using these max and min values, the linear slope of strength vs temperature could then be determined. However, the linear regression is assumed to only occur in the range of 25°C to 300°C, hence the inclusion of constant values for the temperature below 25°C and above 300°C, as seen in the following sets of equations:

- Maximum Tensile Strength (psi) vs. Temperature (°C)

$$\begin{array}{l}
 \circ \text{ Douglas Fir:} \quad \sigma = 1500 \quad \text{for } T \leq 25^{\circ}\text{C} \\
 \quad \quad \quad \sigma = 1500 - 4.308 * T \quad \text{for } 25^{\circ}\text{C} < T < 300^{\circ}\text{C} \\
 \quad \quad \quad \sigma = 0 \quad \text{for } T \geq 300^{\circ}\text{C}
 \end{array} \quad \left. \vphantom{\begin{array}{l} \sigma = 1500 \\ \sigma = 1500 - 4.308 * T \\ \sigma = 0 \end{array}} \right\} (2.1)$$

$$\begin{array}{l}
 \circ \text{ Southern Pine:} \quad \sigma = 2350 \quad \text{for } T \leq 25^{\circ}\text{C} \\
 \quad \quad \quad \sigma = 2350 - 8.217 * T \quad \text{for } 25^{\circ}\text{C} < T < 300^{\circ}\text{C} \\
 \quad \quad \quad \sigma = 0 \quad \text{for } T \geq 300^{\circ}\text{C}
 \end{array} \quad \left. \vphantom{\begin{array}{l} \sigma = 2350 \\ \sigma = 2350 - 8.217 * T \\ \sigma = 0 \end{array}} \right\} (2.2)$$

$$\begin{array}{l}
 \circ \text{ Spruce Pine:} \quad \sigma = 1250 \quad \text{for } T \leq 25^{\circ}\text{C} \\
 \quad \quad \quad \sigma = 1250 - 4.049 * T \quad \text{for } 25^{\circ}\text{C} < T < 300^{\circ}\text{C} \\
 \quad \quad \quad \sigma = 0 \quad \text{for } T \geq 300^{\circ}\text{C}
 \end{array} \quad \left. \vphantom{\begin{array}{l} \sigma = 1250 \\ \sigma = 1250 - 4.049 * T \\ \sigma = 0 \end{array}} \right\} (2.3)$$

- Modulus of Elasticity (psi) vs. Temperature ($^{\circ}\text{C}$)

$$\begin{array}{l}
 \circ \text{ Douglas fir:} \quad E = 1900000 \quad \text{for } T \leq 25^{\circ}\text{C} \\
 \quad \quad \quad E = 1900000 - 3719 * T \quad \text{for } 25^{\circ}\text{C} < T < 300^{\circ}\text{C} \\
 \quad \quad \quad E = 1900000 \quad \text{for } T \geq 300^{\circ}\text{C}
 \end{array} \quad \left. \vphantom{\begin{array}{l} E = 1900000 \\ E = 1900000 - 3719 * T \\ E = 1900000 \end{array}} \right\} (2.4)$$

$$\begin{array}{l}
 \circ \text{ Southern Pine:} \quad E = 1800000 \quad \text{for } T \leq 25^{\circ}\text{C} \\
 \quad \quad \quad E = 1800000 - 5206 * T \quad \text{for } 25^{\circ}\text{C} < T < 300^{\circ}\text{C} \\
 \quad \quad \quad E = 1800000 \quad \text{for } T \geq 300^{\circ}\text{C}
 \end{array} \quad \left. \vphantom{\begin{array}{l} E = 1800000 \\ E = 1800000 - 5206 * T \\ E = 1800000 \end{array}} \right\} (2.5)$$

$$\begin{array}{l}
 \circ \text{ Spruce Pine:} \quad E = 1500000 \quad \text{for } T \leq 25^{\circ}\text{C} \\
 \quad \quad \quad E = 1500000 - 3719 * T \quad \text{for } 25^{\circ}\text{C} < T < 300^{\circ}\text{C} \\
 \quad \quad \quad E = 1500000 \quad \text{for } T \geq 300^{\circ}\text{C}
 \end{array} \quad \left. \vphantom{\begin{array}{l} E = 1500000 \\ E = 1500000 - 3719 * T \\ E = 1500000 \end{array}} \right\} (2.6)$$

Similarly, a linear regression was assumed for the glue types, as that is what best fit as well. However, due to the fact that there is limited mechanical information for the various glue types, such as the modulus or the maximum strength, these values had to be taken from the experimental results. Due to the fact that the test results were normalized against a sample of

solid wood, it's a reasonable assumption that the test values are close to the actual strength and modulus. The method for developing the regression is the same as for wood, however the change comes from determining the glues strength at 25°C, because the glue types were not tested below 100°C. Because the assumption is that the strength and modulus degrade linearly, it is a reasonable to assume that that trendline will continue as the temperature decreases. Thus, the strength was linearly interpolated for room temperature, and is also included in Table 2.2. Therefore, normalization was not required for the linear regression equations. Similar to the equations describing the wood specie's behavior, the glue types had a boundary at the 25°C room temperature as seen on the following sets of equations:

- Maximum Shear Strength (psi) vs. Temperature (°C)

$$\begin{array}{l} \circ \text{ PUR1:} \\ \sigma = 654.5 - 2.54 * T \text{ for } T > 25^\circ\text{C} \\ \sigma = 654.5 \text{ for } T \leq 25^\circ\text{C} \end{array} \quad \left. \vphantom{\begin{array}{l} \sigma = 654.5 - 2.54 * T \text{ for } T > 25^\circ\text{C} \\ \sigma = 654.5 \text{ for } T \leq 25^\circ\text{C} \end{array}} \right\} \quad (2.7)$$

$$\begin{array}{l} \circ \text{ PUR2:} \\ \sigma = 564.3 - 1.72 * T \text{ for } T > 25^\circ\text{C} \\ \sigma = 564.3 \text{ for } T \leq 25^\circ\text{C} \end{array} \quad \left. \vphantom{\begin{array}{l} \sigma = 564.3 - 1.72 * T \text{ for } T > 25^\circ\text{C} \\ \sigma = 564.3 \text{ for } T \leq 25^\circ\text{C} \end{array}} \right\} \quad (2.8)$$

$$\begin{array}{l} \circ \text{ PRF:} \\ \sigma = 707.5 - 2.08 * T \text{ for } T > 25^\circ\text{C} \\ \sigma = 707.5 \text{ for } T \leq 25^\circ\text{C} \end{array} \quad \left. \vphantom{\begin{array}{l} \sigma = 707.5 - 2.08 * T \text{ for } T > 25^\circ\text{C} \\ \sigma = 707.5 \text{ for } T \leq 25^\circ\text{C} \end{array}} \right\} \quad (2.9)$$

$$\begin{array}{l} \circ \text{ MF:} \\ \sigma = 650.4 - 1.90 * T \text{ for } T > 25^\circ\text{C} \\ \sigma = 650.4 \text{ for } T \leq 25^\circ\text{C} \end{array} \quad \left. \vphantom{\begin{array}{l} \sigma = 650.4 - 1.90 * T \text{ for } T > 25^\circ\text{C} \\ \sigma = 650.4 \text{ for } T \leq 25^\circ\text{C} \end{array}} \right\} \quad (2.10)$$

- Modulus of Elasticity (psi) vs. Temperature (°C)

$$\begin{array}{l} \circ \text{ PUR1:} \\ E = 3741980 - 23154 * T \text{ for } T > 25^\circ\text{C} \\ E = 3741980 \text{ for } T \leq 25^\circ\text{C} \end{array} \quad \left. \vphantom{\begin{array}{l} E = 3741980 - 23154 * T \text{ for } T > 25^\circ\text{C} \\ E = 3741980 \text{ for } T \leq 25^\circ\text{C} \end{array}} \right\} \quad (2.11)$$

$$\begin{array}{l} \circ \text{ PUR2:} \\ E = 3118317 - 15289 * T \text{ for } T > 25^\circ\text{C} \\ E = 3118317 \text{ for } T \leq 25^\circ\text{C} \end{array} \quad \left. \vphantom{\begin{array}{l} E = 3118317 - 15289 * T \text{ for } T > 25^\circ\text{C} \\ E = 3118317 \text{ for } T \leq 25^\circ\text{C} \end{array}} \right\} \quad (2.12)$$

$$\begin{aligned} \circ \text{ PRF:} \quad & E = 3741980 - 18710 * T \text{ for } T > 25^{\circ}\text{C} \\ & E = 3741980 \quad \text{for } T \leq 25^{\circ}\text{C} \end{aligned} \quad \left. \vphantom{\begin{aligned} \circ \text{ PRF:} \quad & E = 3741980 - 18710 * T \text{ for } T > 25^{\circ}\text{C} \\ & E = 3741980 \quad \text{for } T \leq 25^{\circ}\text{C} \end{aligned}} \right\} (2.13)$$

$$\begin{aligned} \circ \text{ MF:} \quad & E = 2494654 - 10914 * T \text{ for } T > 25^{\circ}\text{C} \\ & E = 2494654 \quad \text{for } T \leq 25^{\circ}\text{C} \end{aligned} \quad \left. \vphantom{\begin{aligned} \circ \text{ MF:} \quad & E = 2494654 - 10914 * T \text{ for } T > 25^{\circ}\text{C} \\ & E = 2494654 \quad \text{for } T \leq 25^{\circ}\text{C} \end{aligned}} \right\} (2.14)$$

The results from this study are not only beneficial to the work this thesis focuses on but are of great reference value to the further understanding of wood and glue. While there are many more wood species in timber construction, this study serves a baseline for the general understanding of burning wood. The results of the wood tests are fairly straightforward. There were a few outlying patterns but those are differed to as errors in the grain pattern of the wood, at such a small scale. It was determined that ultimate strength and modulus decline in a linear fashion as heat is applied. The results of the shear tests were fairly similar. The PRF adhesive was found to have a reaction similar to solid wood. The other adhesives all noticed a significant decrease in material strength around the 260°C temperature line. Based on these results, a pattern for the strength vs temperature can be determined and applied to the study of CLT in fir conditions. The following section will outline the method of the finite element analysis used in this study.

CHAPTER THREE: RESEARCH METHODOLOGY

3.1 Overview of Modeling Method

As it is revealed in the literature review, the majority of existing studies on CLT fire performance were experimental studies. Most of these studies focused on the combustibility and fire rating of the CLT components. Typically, full burning of the panel was conducted and the performance related to fire engineering, such as heat release and the potential of second flash over due to delamination, was the focus of the study. There is very limited study on the impact of elevated temperature on structural performance, specifically panel strength and stiffness. A common practice is to calculate the reduced cross-section area of CLT based on the exposure time and char rate of wood material, then simply eliminate the wood that has been considered charred. In this study, we seek to develop a more systematic understanding of the transition of CLT panel structural performance from room temperature to the charring of the exposed layer. This is achieved through a detailed 2D model constructed using finite element method (FEM).

There are many advantages of utilizing FEM in a study of this type. The first and foremost being the ability to control element size to enable modeling of different parts in a CLT assembly. The analysis will provide very detailed stress and deformation results over the entire region of the modeled CLT cross section. These simulated responses can then be compared to either the test measured responses (if full-scale testing results are available) or classic closed form solutions that are similar to the situation simulated. Once the FEM approach is validated through data, it will allow for a variety of temperature profiles to be imposed numerically, thus saving resources for testing. In this study, when large scale testing is not available, the use of

computer modeling allows for systematic investigation of CLT panel assembly's under different temperature profile conditions in a reasonable amount of time.

In this study, we are using an open source general FEM program OpenSees. OpenSees, also known as the Open System for Earthquake Engineering Simulation, is an object-oriented software framework. It is used to create serial and parallel finite element computer simulations, that can give the response of either structural or geotechnical systems. Essentially it is a database of solvers and recorders that can efficiently determine the solution to FEM problems [9]. While the OpenSees is originally intended to run complex dynamic analyses, it is more than capable of handling simple static simulations, which is what this study focuses on. Since the OpenSees framework does not have a pre- and post-processing capacity, the overall modeling approach can be broken into three main steps. The first step is creating the various input parameter matrices and values that define the CLT being analyzed. These parameters were stored in Matlab where a program is then developed to create input files for OpenSees to conduct the analysis. This is essentially a customized pre-processing program for this study. Following the Matlab pre-processing, the OpenSees solving engine is called to run the FEM analysis. To the benefit of this process, OpenSees can be set up to be highly automated, running the entire analysis with very little user input. The results of the analysis were then written into result files following the format of OpenSees output. Finally, another post-processing tool was developed in Matlab to import, plot, extract and analyze the resulting data to provide engineering insights.

This entire process and the Matlab programs were developed based on the complexity of the model being analyzed. For the scale of the model under static loading conditions, the average analysis time is around 10 minutes for a given CLT design. Having a tool to run an analysis this quickly is highly beneficial as it allows fast iterations to try a variety of CLT design

and temperature conditions. These tools developed as part of this thesis work enabled the analysis of all possible combinations of wood and glue configurations we have small scale data for, each over a wide range of temperatures. The details on these procedures and the FEM model itself are explained in the subsequent sections.

3.2 Matlab Pre - Processing

In this study, Matlab is used extensively to assist the modeling and interpretation of the analysis results. Specifically, the pre-processing modules were developed as Matlab functions that take in basic CLT panel design and analysis parameters, outputting the needed input files for OpenSees to perform the FEM analysis. The structure selected was a simply supported CLT panel with a 16 ft. span as it is shown in Figure 3.1. This simple CLT floor span will be loaded with a concentrated force at mid-span to develop a deflection. The parameters that control the analysis include:

- CLT span length (L)
- Total CLT panel height (H)
- Thickness of each wood lamination within CLT ($h_1, h_2 \dots h_i$)
- Edge glue (not implemented in most North American CLT panels) interface locations within CLT ($l_1, l_2 \dots l_i$)
- External loading (P): In this study, only a simple concentrated load is added. Because all the analysis done here is linear, the results of the analysis will be fully scalable.
- Size of FEM mesh, in x and y directions (M_x, M_y)
- Material properties, including modulus of elasticity/poissons ratio for wood with grain in parallel and perpendicular direction, and modulus of elasticity/poissons for glue lines.

Note that because of the temperature change, the material of wood and glue will change with the temperature, they are represented by different materials.

- Boundary condition: In this case we use symmetry to reduce the model to a cantilevered half-span model
- Temperature profile: How the temperature is distributed through the CLT.

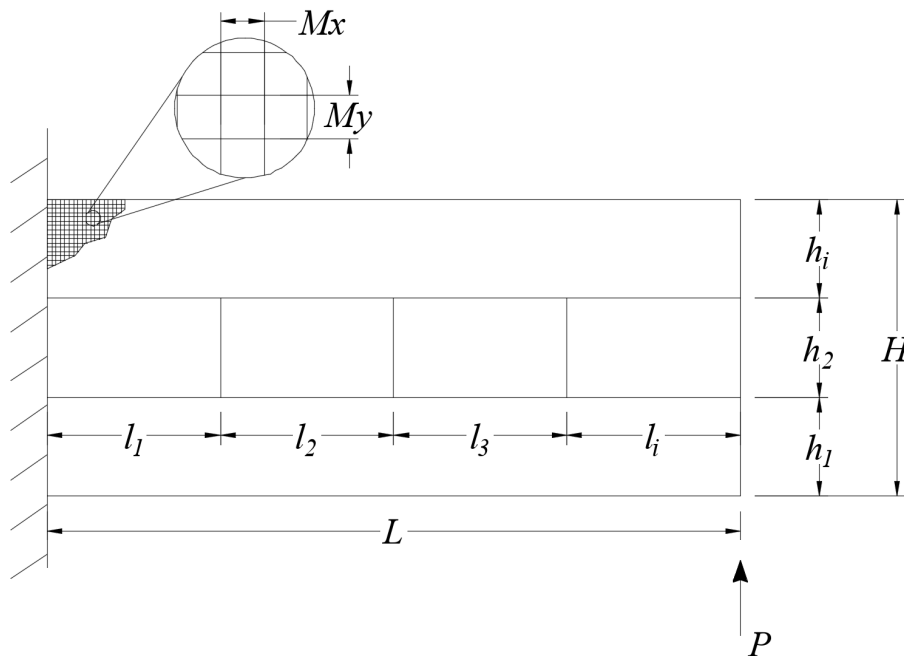


Figure 3.1 CLT Panel Parameters

Note that because the focus of the of this study is the impact of fire and heat, not all of the above parameters will be changed over the models. The following parameters were kept consistent for all the models analyzed in this thesis:

- $L = 8\text{ft}$ (96in) (This means that the whole slab panel has a 16ft span)
- Panel Height, H
 - o 3-Ply $\sim H = 4.5\text{in}$

- 5-Ply $\sim H = 7.5\text{in}$
- 7-Ply $\sim H = 10.5\text{in}$
- $l_1 = 3.5''$, $l_2 = 3.5''$, $l_i = 3.5''$ (Consistent for 5, 7, and 9 Ply's)
- $h_1 = 1.5''$, $h_2 = 1.5''$, $h_i = 1.5''$ (Consistent for 5, 7, and 9 Ply's)
- $P = 500\text{ lbs}$
- $B = 12\text{in}$
- $M_x = 0.0625\text{in}$, $M_y = 0.0625\text{in}$
- Boundary Condition: All nodes fully fixed at left side

The material properties for the wood species and glue types at room temperature were all kept consistent as well. For the wood types, the values were taken directly from the NDS Supplement, specifically Table 4A and Table 4B [10]. The poisson's ratios are not available in the NDS however, so the values were taken from a timber bridge construction manual, which listed poisson's ratios for various wood species [11]. Another property that the NDS doesn't provide is the elastic modulus for wood in its weak direction. In order to determine a value of this to use in the program, the ratio between the compressive strength perpendicular to the grain ($F_{C\perp}$) and the compressive strength parallel to the grain (F_C) was used to reduce the modulus. For the various glue types, the values had to be assumed from the small-scale testing. However, this is a reasonable assumption as both the modulus and shear strength of each glue was significantly higher than the corresponding values for the wood, thus enforcing the accepted understanding that wood glue should be stronger than the wood glue itself at room temperature. The poisson's ratios for the glue was selected to be 0.29 as a consistent

value due to the lack of information on the actual poisson's ratio of the glue values. The constant material properties are summarized in Table 3.1.

Table 3.1 Constant Material Values

Wood Grain in Parallel Direction	Wood Type	E (psi)		Bending Strength (psi)	Poissons Ratio
	Douglas Fir	1900000		1500	0.29
	Southern Pine	1500000		1250	0.33
	Spruce Pine	1800000		2350	0.37
Wood Grain in Perpendicular Direction	Wood Type	F _{c⊥} /F _c Ratio	E (psi)	Bending Strength (psi)	Poissons Ratio
	Douglas Fir	0.37	703000	1500	0.39
	Southern Pine	0.32	480000	1250	0.38
	Spruce Pine	0.30	540000	2350	0.44
Glue Types	Glue Type	E (psi)		Shear Strength (psi)	Poissons Ratio
	PUR1	3741980		654.5	0.29
	PUR2	3118317		564.3	0.29
	PRF	3741980		707.5	0.29
	MF	2494654		650.4	0.29

The parameters that are changed in this study are more complex however. The first parameter being the maximum temperature that the model experiences. The fire in this study is assumed to be applied uniformly over the bottom surface of the model, i.e. the location of the maximum temperature. By changing the input temperature, the structural properties of the panel can be captured at an exact instance. The range of temperatures used in this study is 25°C-300°C, this range being chosen as 25°C is the room temperature of the model, and 300°C is the maximum temperature the wood can reach, as it is generally assumed to char and lose its strength at 300°C, thus this assumption is kept consistent in this study.

The maximum temperature is an important parameter in that it defines the temperature profile that the beam experiences. In this study we utilize two temperature profiles, the first is uniform, like the normal non-heated condition as the baseline, all elements in models have the same temperature. Once fire is added to the model, the panel is no longer in a uniform temperature condition. In order to determine the propagation of heat, we used more test data from previous studies done by FPL (CLT Panel burning tests) to determine the equation to represent the temperature profile. The following figure illustrates the pattern of temperature vs depth of wood. We looked at a set of data for when the bottom of a solid wood member reached char, and assumed an exponential regression, as it fit the data the best. This plot can be seen in Figure 3.2.

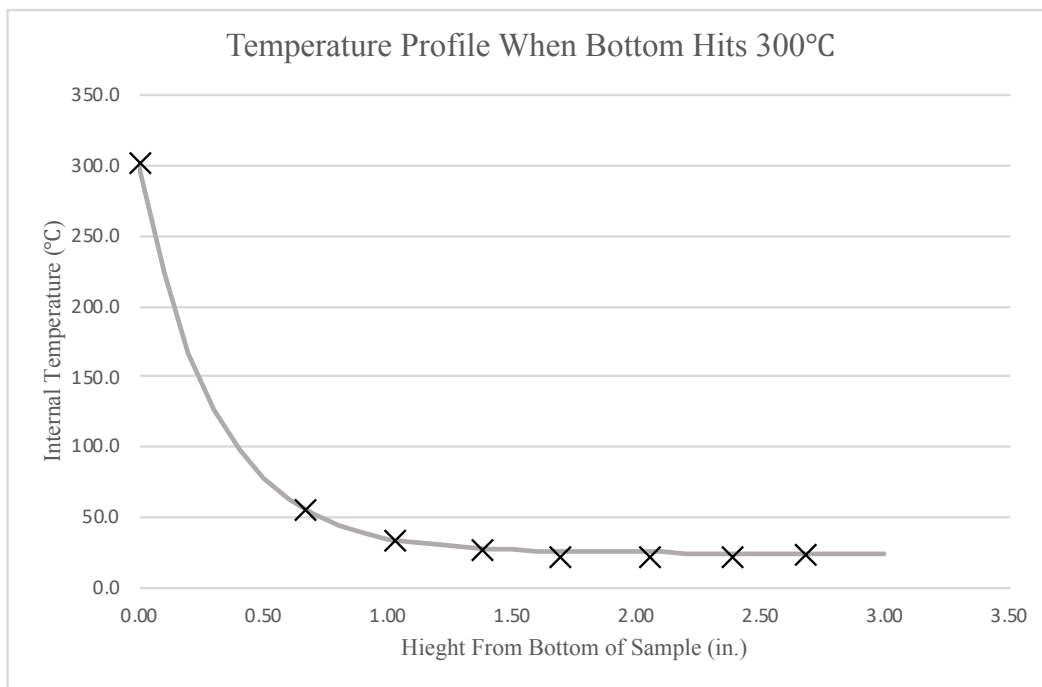


Figure 3.2 Temperature Profile Taken from FPL Experimental Data

The data points shown in Figure 3.2 is the raw data taken from the FPL study by thermal couple measurements embedded in a CLT panel when the bottom of the wood reaches roughly 300°C. The data received from FPL was a measure of temperature at each thermocouple at a specific time. A thermocouple was placed directly on the bottom of the panel; however, this data point was neglected due the effects of direct heating. The data presented in Figure 3.2 was taken from where the first thermocouple probe in the panel reached 300°C. The trendline was verified by developing curves of a few other sets of data a varying temperature. The exponential regression remained consistent regardless of the temperature at the bottom, and thus the set of data presented above was chosen to use for the regression equation. As is evident, an exponential curve fits the plot the best, thus an online curve fitting tool was used to get the equation of the temperature regression [12]. The resulting equation, in terms of maximum temperature is as follows:

$$T = 25 + (T_i - 25)e^{-3.3y}$$

Where T_i is the maximum temperature at the bottom of the panel, and T is the resulting temperature at height y , in °C. The maximum temperature T_i effectively “shifts” the regression so that the value at $y=0$ is equal to T_i , and the regression continues from there.

With all of the parameters fixed, and the temperature/temperature profile assigned to a model, MATLAB outputs the following files (which are needed for OpenSees to run):

- A general Model file in Matlab containing the following information:
 - o General model properties discussed above
 - o Integer values determining the wood and glue type
 - o Material matrix containing values for all materials based on wood and glue selection

- A vector of all nodes and their individual numbers
 - A vector of all elements and their individual numbers
 - A matrix of the x coordinates for all nodes
 - A matrix of the y coordinates for all nodes
 - A matrix of the x coordinates for all elements
 - A matrix of the y coordinates for all elements
 - A matrix containing information for each element (element number, node numbers for each corner, material tag, and thickness)
- NodeCoord.tcl ~ A file listing the node number, and the (x,y) coordinates for each node
 - Materials.tcl ~ A file listing the materials tag number, the modulus E, the poisons ratio, and specific gravity
 - Elements.tcl ~ A file listing the elements tag number, node numbers at each corner, corresponding material tag, and thickness)
 - LoadPattern.tcl ~ A file listing the nodes where a load is applied, the magnitude of the load, and the direction of the load
 - SPConstraints.tcl ~ A file listing the nodes that are constrained, and in which direction the constraints are. Note, in this study, only the nodes at the left end of the panel are fixed to simulate a cantilevered beam. The nodes are fully fixed in the x and y directions.
 - Recorder.tcl ~ A file listing which nodes and elements will have recorded data
 - AnalysisOptn_1.tcl ~ A file listing the various options to run the analysis in OpenSees

When the creation and output of these files is completed, the analysis is then passed to OpenSees.

3.3 Finite Element Modeling

Since the CLT panel is essentially a one-way slab with different materials at different layers, it is common to reduce this problem to a 2D FEM model. Essentially, we further used symmetry about the center of the slab in order to reduce a 16ft span simply supported slab (16ft is a relatively common span for such applications) to an 8ft cantilevered beam. Then we used a 2D plane-strain element to represent a slice of the slab.

OpenSees has a generalized 2D element “quad” that can be used. In order to define the model and obtain correct outputs, the following information regarding the element must be provided:

- The element tag number to identify where and what the element is
- The four nodes defining the element boundaries, iNode - lNode
 - o These must be input in a counter clockwise direction around the element
- The element thickness in the z direction. For this study, the thickness of the element is the depth of the cantilever beam, which remains constant at 12in
- The type of element that is being used to define the material behavior. In this study it is set to be a “PlaneStrain” element due to the slab geometry constraints.
- The material tag number of the element. This defines the material properties of each individual element, as defined below.

In order to accurately simulate the slab bending behavior and obtain enough accuracy and density in the output, we use 0.0625in x 0.0625in as the basic element size. Chapter 2 details the determination of this sizing choice. This means for a 96in x 4.5 in model, there will be a total of

112201 nodes, and 110592 elements. Within these elements, the different materials are defined by a material tag number (the values of which can be found in Table 3.1):

- 1: This tag number represents the “gap” between the edges of the middle layers.
 - o Although there are some CLT manufacturers in Europe that use edge glue in the middle layers, it is typically not implemented by American manufacturers. This gap is modeled using a material that is very weak (i.e. a gap) and that doesn’t change with temperature.
- 2: Wood with grain in strong direction of loading, in this study the grain runs in the x direction. This is a material property that changes with temperature.
- 3: Wood with grain perpendicular to strong direction of loading, in this study the grain runs in the z direction (out of plain). This is a material property that changes with temperature.
- 4: The glue in between layers, which is only a single row of elements.

An illustration of a typical model, with the different material types is conceptually shown in Figure 3.3. The light blue represents the wood in its strong direction, while the green represents wood in its weak direction. Similarly, they yellow layers represent the glue layer, while the dark blue represents the “gap” material of the non-glue interface. Note that the Figure shows where the materials are in the different regions, however, the grid displayed here is not to scale with the real size of the model (as it will not be able to fit in the printed page. The displayed ratio of span and thickness is not accurate). Furthermore, this plot does not show the individual elements due to the small size compared to the scale of the overall plot. Figure 3.3 is displayed as a

conceptual demonstration of the panels cross section, to lend to a better understanding of the model creation.

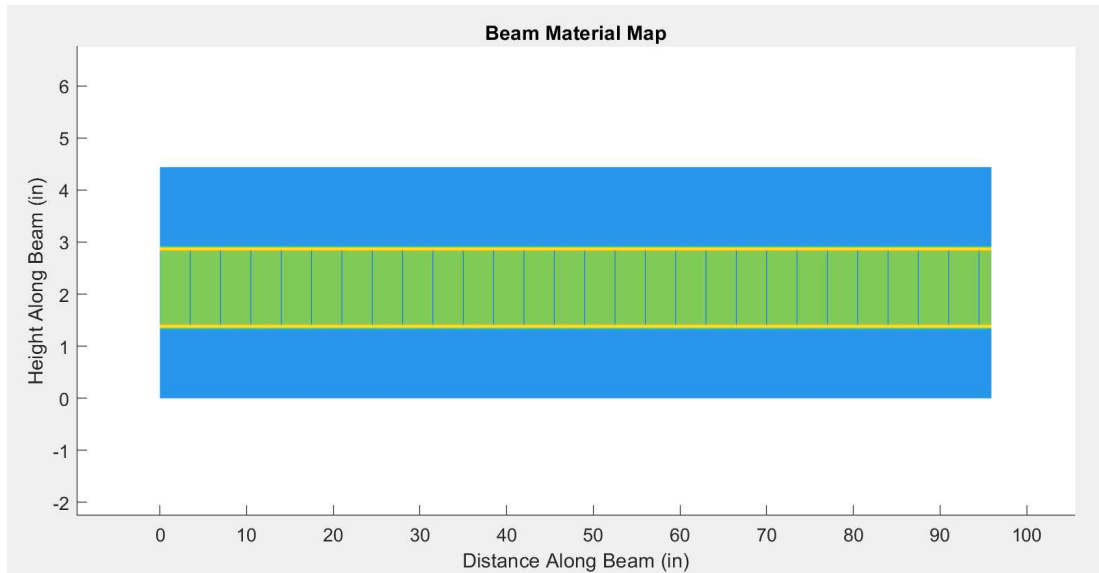


Figure 3.3 Material Map of CLT Panel Slab

In the case of adding heat to the model, the material properties at the elements with increased temperatures need to be adjusted. For every vertical row of elements, the height at the center of the element is known, which is then input into the temperature profile curve to get the exact temperature for that element. Then the material properties are determined using the linear regression equations, and these are appended onto the material matrix defined in the Model array. All the processes are automated using Matlab. Matlab then runs through the element matrix containing the material matrix and increments every row by a value of 4 x the rows locations. This means that the materials assigned before are stay in the correct spot, but the material strength decreases as the tag number increases,

Once the Matlab code is set up, it is easy to manipulate the material property to each element in the predefined grid. This makes it easy to overlay a variety of fire/temperature patterns by assigning different materials (with adjusted stiffness values according to the test results) based on the desired temperature at various regions. The wood and glue material experiencing higher temperatures are essentially weakened in the analysis based on the assigned temperature. As described earlier, a set of Matlab functions were developed to generate the needed input files that represent the model and the corresponding temperature patterns. Then OpenSees runs the simulation and the nodal and element responses for stress strain and displacement.

3.4 Post-Processing

The OpenSees analysis generates a series of output files containing the results of the designated parameters as set by the Matlab pre-processing programs. All of the raw data was recorded to individual .txt files, corresponding to their contents, as follows:

- Disp_Node_X.txt ~ Contains the x direction displacement for all nodes
- Disp_Node_Y.txt ~ Contains the y direction displacement for all nodes
- Element_Strains.txt ~ Contains strains for the four nodes of an element, each broken into strain in x (ϵ_x), strain in y (ϵ_y), and shear strain (γ_{xy})
- Element_Stress.txt ~ Contains stresses for the four nodes of an element, each broken into shear in x (σ_x), shear in y (σ_y), and shear stress (τ_{xy})
- Node_Reaction_X.txt ~ Contains the nodal reactions in x for all nodes
- Node_Reaction_Y.txt ~ Contains the nodal reactions in y for all nodes

These files are saved in ASCII format; thus, they require extraction and post-processing through other Matlab programs. One of the challenges of extracting the data was determining how to convert the raw data into usable matrices and vectors. There was specifically a challenge in regard to the element stress and strain result files. OpenSees records the “element” reactions by taking the reactions for the four nodes that make up the perimeter of the element. Because of this, each element has four different values. In order to account for this, the nodal average was taken for each element, thus condensing the result matrix into one that matches the dimensions of the panel segment. This was done for both the stress and strain output files.

Due to the specialty of this study, a dedicated post-processing program was developed in Matlab, that can extract the data from these files and store them in matrices and vectors usable in Matlab. The program also has the ability to further visualize and analyze the results with a graphical user interface shown in Figure 3.4 (page 33).

As shown in Figure 3.4 (page 33) there are initially seven different functions that the program will execute. In the case of the “Numerical Data” and “Visual Data (Plots)” options, they further direct the user to sub menus where more specific data can be selected. The individual functions of each are described in more detail as follow:

- Main Menu:
 - o Create Model: This function is a part of the pre-processing step. It generates the Model array used in Matlabs workspace, filling the data as discussed in Section 3.2 of this thesis. It generates the data based on the parameters entered into Matlab prior to running.

- Write TCL file for OpenSees: This function is part of the pre-processing step. It takes the Model from the workspace and writes the .tcl files needed to run the OpenSees Analysis.
 - Import Data to Workspace: This is the initial, and largest step in the post-processing portion. This will read the output .txt files generated by OpenSees and import them into the Matlab workspace as the Results array. While importing the data, it simultaneously extracts everything into the desired matrices and vectors, so the Results array is ready to use and requires not further alteration.
 - Add Fire Conditions to Model: This function is part of the pre-processing step when fire is to be included in the analysis. Similar to the “Create Model” option, this function generates the Fire array in the Matlab workspace, create the necessary values to overlay the fire conditions onto the panel. It also modifies the original Model array to include the material properties at elevated temperatures, as well as the matrix that assigns the material tags to the elements. This run after the model is created, to ensure that the data is written properly.
- Numerical Data Sub-Menu: This option, as seen in Figure 3.4 leads the user to a sub menu which options will complete the following:
- Display Min/Max Values: This will take the user to another menu that prompts what numeric values to display. Generally, the “Display All” option is the best, but the min/max values for individual cases can be displayed as well. The values that are displayed are displacement, nodal reactions, stresses in both directions with shear stress, and strain in both directions with shear strain.

- Determine Values at Node: In the case that a specific node is being analyzed, this option will allow the user to input the node number, and the values of that specific node will be determined.
 - Export Values to Workspace: In the case that the min/max values of the panel are needed in the workspace, this function assigns them to an array.
 - Export to .txt File: In order to save the numeric data, this option will generate a .txt file on the user's desktop containing all the min/max values.
- Visual Data Sub-Menu: This option, as seen in Figure 3.4 leads the user to a sub menu which options will complete the following:
- Stress in X Direction: Plots a contour of the internal stresses in the x direction, overlaid on the panels shape.
 - Stress in Y Direction: Plots a contour of the internal stresses in the y direction, overlaid on the panels shape.
 - Shear Stress of Elements: Plots a contour of the internal shear stresses overlaid on the panels shape.
 - Strain in X Direction: Plots a contour of the internal strain in the x direction, overlaid on the panels shape.
 - Strain in Y Direction: Plots a contour of the internal strain in the y direction, overlaid on the panels shape.
 - Shear Strain of Elements: Plots a contour of the internal shear strain overlaid on the panels shape.
 - Deflection Plot: Plots the over displacement of the panel in a solid color.

- X Displacement Contour: Plots a contour of the nodal displacement in the x direction, overlaid on the original panels shape.
- Y Displacement Contour: Plots a contour of the nodal displacement in the y direction, overlaid on the original panels shape.
- Displacement Magnitude Contour: Plots a contour of the nodal displacement magnitude overlaid on the original panels shape.
- Panel Material Map: Plots a contour of the material tag overlaid on the panels original shape.

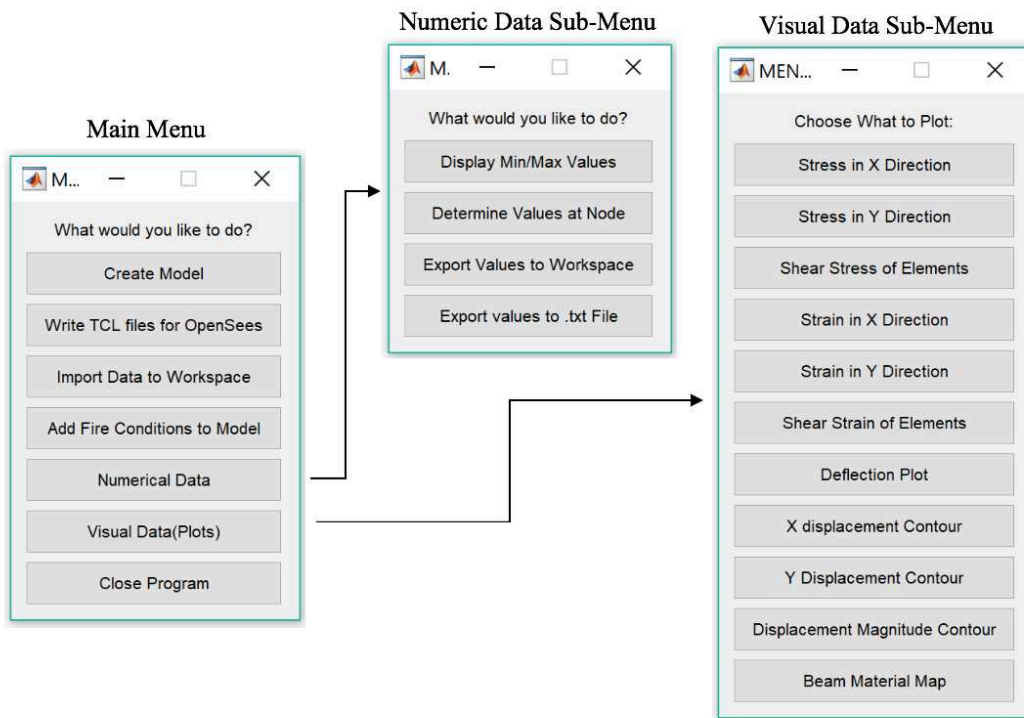


Figure 3.4 Matlab Post-Processing Menu's

3.5 Model Validation

There are many ways to model a bending plate and not all approaches are equal. In order to validate the accuracy of the numerical model, a comparison of the model simulation result and a full-scale testing condition would be ideal. However, full-scale testing of a CLT panel in bending is not available to this study. Thus, we will try to validate the model by comparing the behavior of the FEM model to classic mechanics of materials solutions of a beam. To verify this modeling method produces results similar to the theoretical values, an example beam made of a uniform material (i.e. not layered as CLT) is investigated first. This was done because there is a classic solution for this type of structure.

3.5.1 Solid Wood Beam Bending

To verify the results of this study, the following was tested:

- Douglas Fir wood species $E = 1900000$ psi
- Cantilevered end condition
- 6 inches tall, by 12 inches wide, by 96 inches in length
- 1000 lbs point load at end of beam

In order to determine the beams maximum deflection, only the I value of the cross section needs to be calculated.

$$I = \frac{1}{12}bh^3 = \frac{1}{12}(12 \text{ in.})(6 \text{ in.})^3 = 216 \text{ in.}^4 \quad (3.1)$$

Utilizing the equation for a cantilevered beam, the following is found:

$$Max\ Disp = -\frac{PL^3}{3EI} = -\frac{(1000\ lbs) * (96\ in.)^3}{3 * (1900000\ psi) * (216\ in.^4)} = 0.718596\ in. \quad (3.2)$$

Using the programs developed for this study, with a mesh size of 1 in. x 1 in. the deflection is determined to be 0.7105. Overall, this is a fairly accurate result, having only a 1.12% error. This verifies that the FEM method will yield results that are similar to the theoretical values.

Another important assumption to discuss is the usage of a cantilevered model as opposed to a simply supported model. A simply supported model is the end condition that a one-way CLT slab panel will most commonly be subjected to, however for this study the cantilevered condition will be used to run the analyses. The reason for using the cantilever condition is due to the runtime and efficiency of the coding. By splitting the beam in half, it is effectively cutting the number of nodes and elements in half, allowing the code to run faster while at a smaller element size. In order to justify this assumption, the theoretical deflection using the equation for a simply supported beam can be calculated. Note, both the length and load on the beam is doubled to model the entire beam.

$$Max\ Disp = -\frac{PL^3}{48EI} = -\frac{(2000\ lbs) * (192\ in.)^3}{48 * (1900000\ psi) * (216\ in.^4)} = 0.718596\ in. \quad (3.3)$$

The theoretical values between the two turn out to be identical values, justifying the assumption to use half of a beam in a cantilever condition. The following section will elaborate further on the effects of mesh size on the model.

3.5.1 Determination of FEM Mesh size

One important aspect of this analysis is the size of each individual element in the finite element analysis portion. Variations to the mesh size theoretically should only impact the results by a negligible amount, however, the mesh size will have large impacts on the run time of the program. While this also seems like small factor in the larger scope of this research, the run time per beam has a large impact on the number of tests that can be run and processed over all. In order to test the size and the results it gathered, a test was run in comparison to the ideal results of a beam, determined in the previous section. The same beam parameters were used with the only variable changing being the element size. To test a range of sizes, the elements were started at 2 in. x 2 in. The size was decreased by a factor of 2, until of the size was small enough that the software was over loaded and crashed. Table 3.2 displays the calculated displacement compared to the theoretical displacement for a range of FEM mesh sizes.

Table 3.2 Summary of FEM Mesh Size Tests

Mesh Size (in. x in.)	Displacement (in.)	Theoretical Displacement (in.)	Percent Error
1	0.710537	0.718596	-1.12156
0.5	0.718006	0.718596	-0.08217
0.25	0.719947	0.718596	0.18794
0.125	0.720485	0.718596	0.26281
0.0625	0.720668	0.718596	0.28827
0.03125	0.720763	0.718596	0.30149

This table has quite a few notable traits. The first and foremost being the incredibly small error between the theoretical values and the resultant values from the FEM program. Interestingly enough, the percent error does not converge (or appear to converge) to the

theoretical displacement. Rather, it seems to converge at a displacement at a value just slightly larger than the theoretical value. However, this is still a negligible amount as the largest percent error is still roughly 1.12%. Based on these observations, the ideal element size can be selected based on the percent error that is closest to zero. In this case, the ideal and most efficient element size would be 0.5 inches. However, having a size this large would not work well as fire conditions and glue lines are added to the beam.

As discussed in the methodology of this project, the element size of the glue lines and non-glued interfaces are consistent with the element size of the wood. Therefore, it is highly unrealistic to use an element size that would cause the glue lines to be half an inch thick. Based on this limitation from the coding, a smaller element size should be selected. This was chosen to be 0.0625 inches because it gives a size that is relatively close to the actual thickness of glue in CLT panels.

3.5.3 Layered beam with very weak coupling

Because the modeling of CLT is hinged on the simulation of the layered beam behavior, it is also important to try to validate the simulation using another extreme case where the bonding between beam layers is very weak. For this analysis, we are looking to see if the layers will slip relative to each other while remaining plane, and the deflection of the beam will be larger. In order to achieve this, we set up a 3-layered beam with the following parameters:

- Douglas Fir wood species $E = 1900000$ psi
- Cantilevered end condition
- 6 inches tall, by 12 inches wide, by 96 inches in length
- 1000 lbs point load at end of beam
- Layer heights of $h_1=2$ in, $h_2=2$ in, and $h_3=2$ in.

With the assumption that the glue layers have effectively no strength, the beam deflection can be determined by taking the total load and dividing it into each layer. Then a single layer can be analyzed using the classic beam equation. The following calculations determine the theoretical deflection of the beam.

$$I = \frac{1}{12}bh^3 = \frac{1}{12}(12 \text{ in.})(2 \text{ in.})^3 = 8 \text{ in.}^4 \quad (3.4)$$

$$\text{Load per Layer, } P_l = \frac{P}{3} = \frac{1000 \text{ lbs}}{3} = 333.33 \text{ lbs} \quad (3.5)$$

$$\text{Max Disp} = -\frac{P_l L^3}{3EI} = -\frac{(333.33 \text{ lbs}) * (96 \text{ in.})^3}{3 * (1900000 \text{ psi}) * (8 \text{ in.}^4)} = 6.467303747 \text{ in.} \quad (3.6)$$

After determining the deflection based on the closed equation, the simulation can be run. The deflection calculated through the FEM analysis is 6.177230 in. While this value is not exactly the same, it is still very close to the theoretical value, having a percent error of around 4%. The reason for the error in this situation is that the model still considers the glue lines to be a non-zero material, as OpenSees cannot treat an element as an “empty space”. The modulus of elasticity for the two glue layers is set to be 1 psi, which still has a slight impact on the behavior of the model. In order to validate that the model is appropriately applying the glue layers and considering them, the deflection beam is shown in Figure 3.5 (page 39) while Figure 3.6 (page 39) displays an enhanced view of the beams end, in order to fully demonstrate the expected behavior of the different layers.

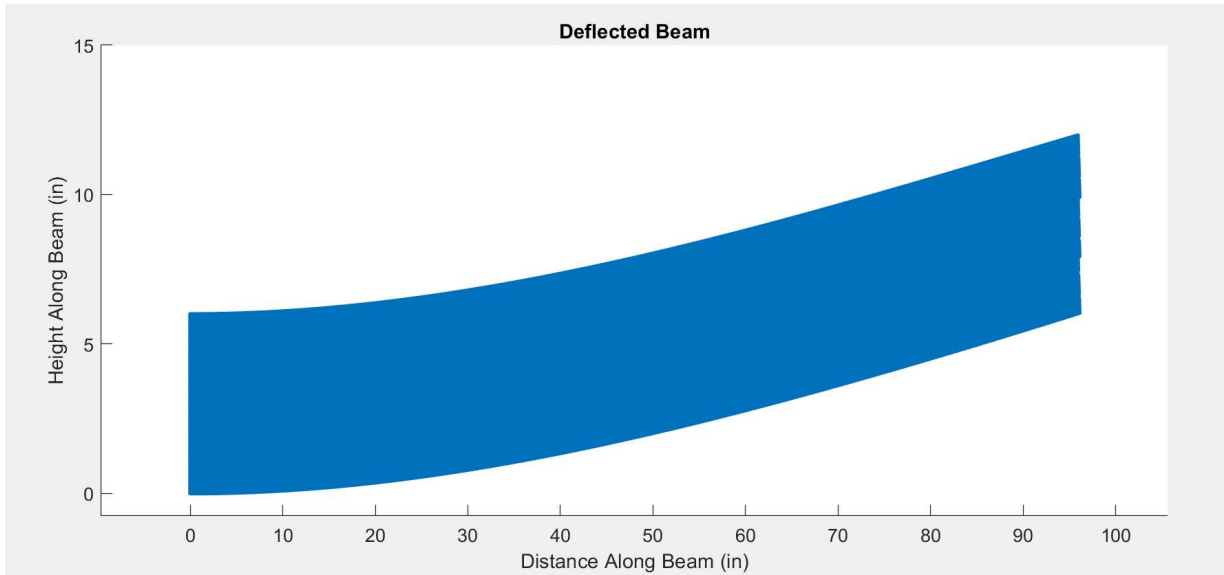


Figure 3.5 Deflection of Beam with Weak Coupling

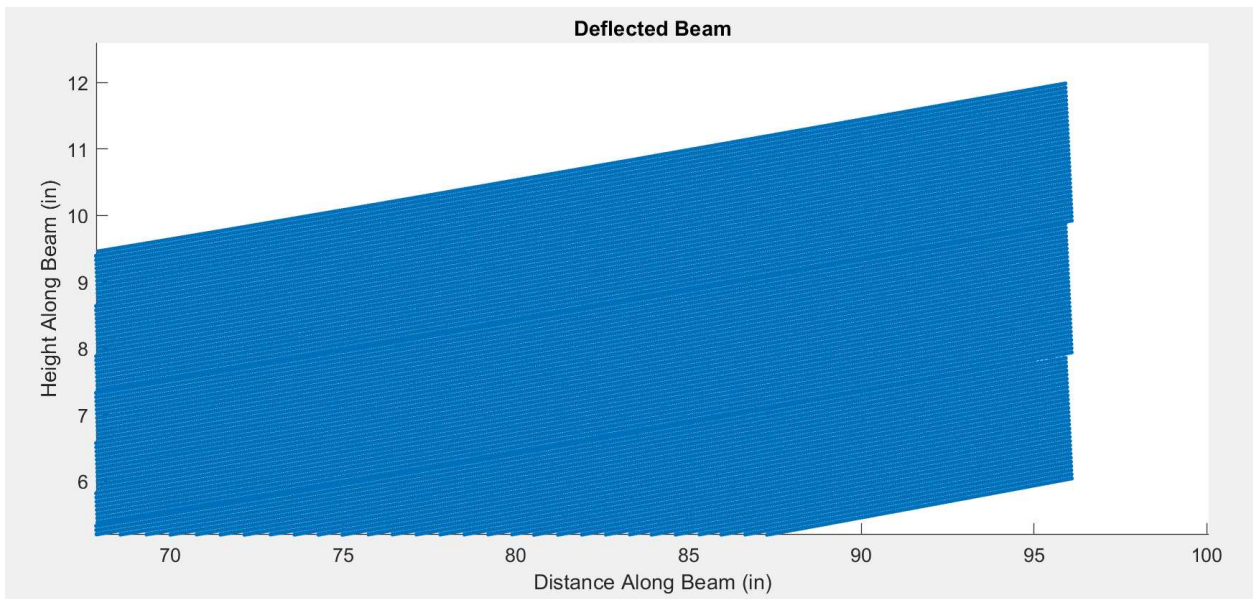


Figure 3.6 Enhanced View of Beam's End with Weak Coupling

The expectation for a layered beam with weak glue lines, is that it will really behave as three individual beams stacked on top of one another. This means that the ends of the beam will

rotate independently of each other, allowing slippage. This can be seen in Figure 3.5 to some extent, however Figure 3.6 provides an enhanced view of the end of the beam to showcase the extent of the slippage. The slippage between two layers is no more than an inch, however this underlines the amount of strength adhesives provide in a layered material. In order to validate the programming correctly applies the materials, the shear strain of the beam is seen in Figure 3.7.

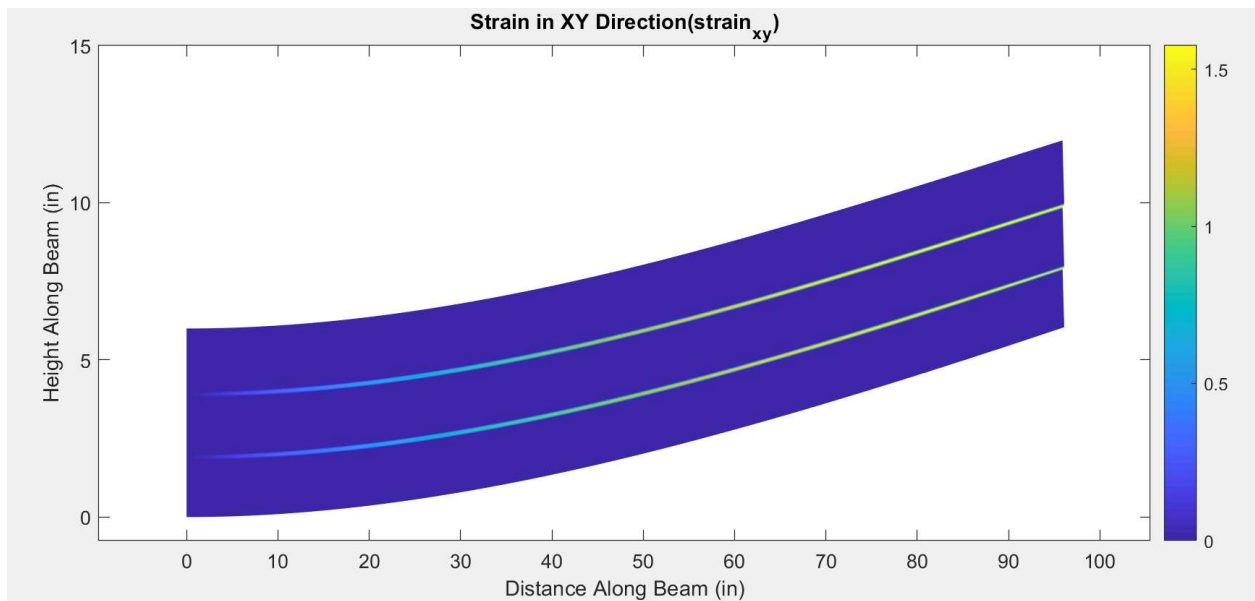


Figure 3.7 Shear Strain of Beam with Weak Coupling

As is seen in Figure 3.7, the layered beam behaves as expected in terms of internal force. The wood layers experience little to no strain under bending, while the elements representing the zero strength layers experience large amounts of strain. This is again consistent with the expected behavior of a beam of this type.

CHAPTER FOUR: CLT PERFORMANCE UNDER ELEVATED TEMPERATURE

4.1 Methodology

The main focus of this study is determining the change in structural properties over a range of temperatures. The first step in accomplishing this is applying the temperature profile of a fire onto the panel in order to accurately detail the precise panel properties at a given temperature. This process is fairly straightforward in terms of the Matlab preprocessing. The first step is to determine develop an expanded matrix of the material properties, containing the material properties at a specific temperature, determined from the temperature profile. Each element in the panel has a specific height, thus the specific temperature at each element is known. A vector is calculated using exponential regression equation listed in section 3.2. The base temperature is input first, then Matlab populates the vector with the temperature at a step size of the FEM Mesh height, M_y . The material matrix is expended by a factor of four times the number of rows in the model. For example, a model with 10 rows of element would have an expanded material matrix of 4×44 , where each column is the material properties at the given height of an element. A function then alters the material tag number element to represent the changed material properties after the elevated temperatures are applied. The temperature step vector is then used in combination with the linear regression equations for each material, developed earlier in this study, to generate two matrices, one containing the temperature dependent modulus of elasticity at every element, while the other one contains the temperature dependent maximum stress at every element.

Once the analysis is run, the next step is to post process the data. This is identical to post processing for a not burned panel, however the biggest change is determining the locations and values of elements that reached or exceeded their limiting stress. To do this, Matlab effectively

“searches” through every single element and compares them the same element in the maximum stress matrix that was created in the pre-processing step. If there is a location where the stress from the analysis is larger than the allowable stress, then Matlab will first, output if it was the wood or glue that reached the limit stress, then calculate the maximum load the model could’ve taken, by using the ratio of the allowable stress to the maximum stress. This will provide insight into how much the applied load should be increased or decreased in order to hit the limiting stress in the panel. The reason for finding the limiting stress and load is that we currently do not have data of full-scale testing for panel capacity. The limiting stress and load are found in order to determine the relative robustness of the different combinations. However, if no element reaches its limiting stress, then Matlab simply outputs the maximum load that the panel could handle and displays “Okay” for the limiting material. This meaning that the beam is okay in terms of limiting stress for the given conditions, however it could still reach the limits under different circumstances. It is also worth noting that for the glue elements, the shear stress is used, whereas the stress in the x direction is used for the wood, as these are the modes by which the glue and wood will likely fail. Having developed a function set of codes to apply and analyze elevated temperatures, the analyses were run.

The first step was to examine the 12 different combinations of wood and glue, to see the variances in the combinations, starting at a room temperature of 25°C to the maximum temperature of 300°C. The temperature was incremented in five steps of 55°C, in order to develop a loose understanding of the how each panel behaves under increasing temperatures. From this, the weakest combinations can be selected, in order to run a sensitivity analysis on how the structural properties change as the number of ply’s are increased, specifically 5-ply and 7-ply CLT panels. The initial testing matrix is shown in Table 4.1, where the individual models are

defined by a naming scheme “Ply Count.Wood#.Glue#.Temperature” shown in Table 4.1, while Table 4.2 shows the testing matrix.

Table 4.1 Naming Convention for Wood and Glue

Naming Conventions for Wood and Glue			
Douglas Fir	1	PUR1	1
Southern Pine	2	PUR2	2
		PRF	3
Spruce Pine	3	MF	4

Table 4.2 First Stage CLT Testing Matrix

Wood and Glue Combination	25°C	80°C	135°C	190°C	245°C	300°C
Douglas Fir/PUR1	3.1.1.025	3.1.1.080	3.1.1.135	3.1.1.190	3.1.1.245	3.1.1.300
Douglas Fir/PUR2	3.1.2.025	3.1.2.080	3.1.2.135	3.1.2.190	3.1.2.245	3.1.2.300
Douglas Fir/PRF	3.1.3.025	3.1.3.080	3.1.3.135	3.1.3.190	3.1.3.245	3.1.3.300
Douglas Fir/MF	3.1.4.025	3.1.4.080	3.1.4.135	3.1.4.190	3.1.4.245	3.1.4.300
Southern Pine/PUR1	3.2.1.025	3.2.1.080	3.2.1.135	3.2.1.190	3.2.1.245	3.2.1.300
Southern Pine/PUR2	3.2.2.025	3.2.2.080	3.2.2.135	3.2.2.190	3.2.2.245	3.2.2.300
Southern Pine/PRF	3.2.3.025	3.2.3.080	3.2.3.135	3.2.3.190	3.2.3.245	3.2.3.300
Southern Pine/MF	3.2.4.025	3.2.4.080	3.2.4.135	3.2.4.190	3.2.4.245	3.2.4.300
Spruce Pine/PUR1	3.3.1.025	3.3.1.080	3.3.1.135	3.3.1.190	3.3.1.245	3.3.1.300
Spruce Pine/PUR2	3.3.2.025	3.3.2.080	3.3.2.135	3.3.2.190	3.3.2.245	3.3.2.300
Spruce Pine/PRF	3.3.3.025	3.3.3.080	3.3.3.135	3.3.3.190	3.3.3.245	3.3.3.300
Spruce Pine/MF	3.3.4.025	3.3.4.080	3.3.4.135	3.3.4.190	3.3.4.245	3.3.4.300

An example of the naming convention for better understanding, 3.1.4.080 is the name of a 3 ply, Douglas Fir and MF glue model tested at 80°C. This naming system is useful not only for the organization of testing, but also for data presentation and discussion in this paper. Once the results for each combination is obtained, the two weakest combinations, as well as the strongest will be test with 5 and 7 ply configurations.

4.2 Verification of Methodology

In order to validate the results of this study, the fire portion of the Matlab programming must also be verified. In order to show this, a contour of each elements modulus of elasticity can be plotted in order to see where the elements with lowered stiffness are located. This is presented in the following figure.

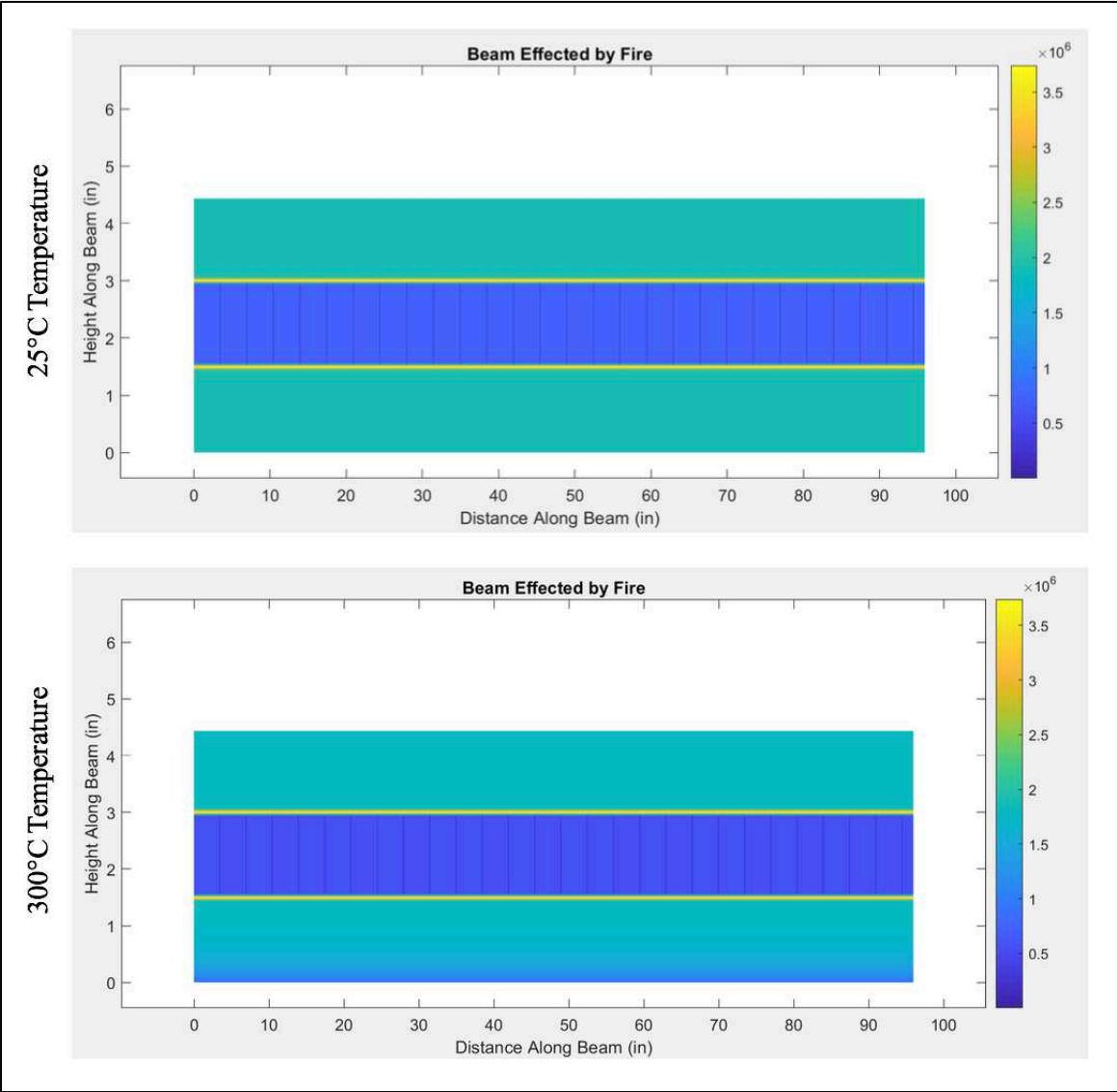


Figure 4.1 Comparison of Room Temperature Panel and Fully Burned Panel

As seen in Figure 4.1 (page 44), the fire overlay portion of the Matlab coding does work. However, based on the temperature profile, the impact of the fire on the panel is very miniscule, only impacting about an inch of wood in the panel model. The dark color on the bottom of the second panel plot is representative of the significant temperature change, which quickly returns to normal the higher in the panel this goes. It is expected that the results from the fire will have a relatively small difference in comparison to one another, however every model is run using this temperature profile, to get results that are accurate to the data used in this study. The next section will discuss the overall effects that the fire does have on the panel.

4.3 Effects of Temperature on Panel Properties

After running the first set of models as shown in Table 4.1, a variety of data was collected. In order to present it in a coherent manner, as well as determine the weakest models to use in further tests, the data was broken into four main parts. The first is the maximum deflection the panel experiences as the temperature is increased. This trend is seen in Figure 4.1 (page 46).

There are a few trends worth noting from this set of data. First and foremost is the overall linear trend the models exhibit over the temperature range. This is to be expected as the material properties were assumed to have a linear regression in strength compared to temperature. The next observation is how minimal the difference between glue types are for a given wood, while the wood types themselves exhibited a noticeable difference in performance. The wood types are seen as Spruce Pine as (wood type 3) the top cluster, Southern Pine (wood type 2) as the middle cluster, and Douglas Fir (wood type 1) as the bottom cluster, while the specific glue types remain clustered in the same area. From this information alone, the southern pine exhibits the most displacement, suggesting that models using this wood will have the

weakest performance. However, the rest of the model's results must be considered. The next set of data to consider is the models limiting material, compared to maximum load that could be applied. The relationship between these two is displayed in Table 4.3 (page 47). For a given model and temperature, the maximum load is displayed as well as the material that will reach its allowable stress at the specified load.

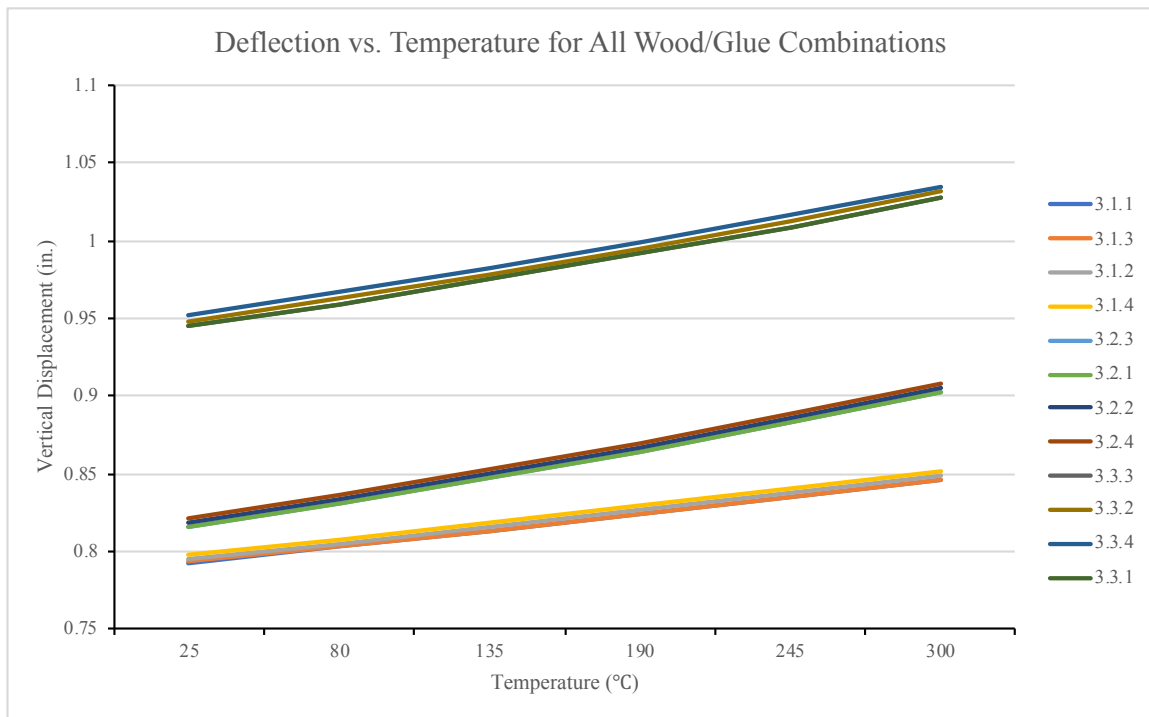


Figure 4.1 Deflection Curves of Varying Wood and Glue Combinations

The biggest trend here is that the wood is consistently the material reaching failure. This occurs regardless of the glue or temperature that is applied. This suggests that even at elevated temperatures, the glue types maintain a higher shear strength than the wood itself. Additionally, the trend in the overall strength of the woods can be seen too. Every model using Southern Pine showed the highest strength in comparison to the other two wood types. In order to understand

how this maximum load changes with temperature, the maximum load was normalized to the 25°C load in order to determine the percent reduction at each temperature. This is seen in Table 4.4.

Table 4.3 Stress Limit Target Load and Limiting Material at Specified Temperatures

Model Number	Stress Limit Target Load at Specified Temperature (lbs) and Limiting Material											
	25°C		80°C		135°C		190°C		245°C		300°C	
3.1.1	430.5	Wood	427.6	Wood	424.6	Wood	421.5	Wood	418.4	Wood	415.2	Wood
3.1.2	429.2	Wood	426.3	Wood	423.3	Wood	420.3	Wood	417.2	Wood	414.0	Wood
3.1.3	430.5	Wood	427.6	Wood	424.6	Wood	421.5	Wood	418.4	Wood	415.2	Wood
3.1.4	427.9	Wood	425.0	Wood	422.0	Wood	419.0	Wood	415.9	Wood	412.7	Wood
3.2.1	708.0	Wood	701.0	Wood	693.7	Wood	686.1	Wood	678.2	Wood	670.0	Wood
3.2.2	705.9	Wood	698.9	Wood	691.5	Wood	684.0	Wood	676.2	Wood	668.1	Wood
3.2.3	708.0	Wood	701.0	Wood	693.7	Wood	686.1	Wood	678.2	Wood	670.0	Wood
3.2.4	703.7	Wood	696.7	Wood	689.5	Wood	682.0	Wood	674.2	Wood	666.2	Wood
3.3.1	302.3	Wood	299.7	Wood	296.9	Wood	294.1	Wood	291.2	Wood	288.2	Wood
3.3.2	301.3	Wood	298.6	Wood	295.9	Wood	293.1	Wood	290.2	Wood	287.3	Wood
3.3.3	302.2	Wood	299.7	Wood	296.9	Wood	294.1	Wood	291.2	Wood	288.2	Wood
3.3.4	300.2	Wood	297.6	Wood	294.9	Wood	292.1	Wood	289.3	Wood	286.3	Wood

Table 4.4 Reduction in Stress Limit Target Load at Varying Panel Temperatures

Model Number	Percent Reduction in Stress Limit Target Load					
	25°C	80°C	135°C	190°C	245°C	300°C
3.1.1	0.00	-0.68	-1.38	-2.09	-2.82	-3.57
3.1.2	0.00	-0.68	-1.37	-2.08	-2.81	-3.55
3.1.3	0.00	-0.68	-1.38	-2.09	-2.82	-3.57
3.1.4	0.00	-0.67	-1.36	-2.07	-2.79	-3.54
3.2.1	0.00	-0.99	-2.03	-3.10	-4.21	-5.37
3.2.2	0.00	-1.00	-2.04	-3.10	-4.21	-5.36
3.2.3	0.00	-0.99	-2.03	-3.10	-4.21	-5.37
3.2.4	0.00	-0.99	-2.02	-3.08	-4.19	-5.33
3.3.1	0.00	-0.88	-1.79	-2.72	-3.68	-4.67
3.3.2	0.00	-0.87	-1.78	-2.71	-3.66	-4.65
3.3.3	0.00	-0.85	-1.75	-2.69	-3.65	-4.64
3.3.4	0.00	-0.87	-1.77	-2.69	-3.64	-4.63

Looking at the change in maximum loading over the temperature range, the over all reductions per temperature remain fairly consistent across the various combinations. They follow a general linear trend in the reduction of the maximum load, is expected as the material properties used an assumed linear reduction versus temperature. Another observation is the relatively low magnitude of the limit state loads in Table 4.4 (page 47). The reason for these values is because they are developed directly using allowable stress values from the NDS which uses built in factors of safety. The values presented in this table should not be confused with failure loads, but rather the loads when the beam will reach its limiting allowable stress. Finally, the stiffness of the models can be determined at a given temperature as displayed in Table 4.5 (page 49). Similarly, Table 4.6 (page 49) displays the same data, however it visually categorizes each model's stiffness at a given temperature.

Overall, the trend of spruce pine remains the same as these models exhibiting the lowest stiffness. Not only is the initial stiffness of spruce pine the lowest, it also shows the biggest drop in strength over the temperature range, dropping by nearly 90 lbs/in. On the contrary, Douglas Fir maintains the trend of being the strongest wood type, have the highest initial stiffness, and small drop in stiffness of only 40 lbs/in. In term of the southern Pine wood, it showcased a similar initial stiffness and stiffness change to that of Douglas Fir. This is important to note, as southern pine showed the highest strength and maximum load, while being second in stiffness. If anything, this showcases the ductility of southern pine as a wood species.

Comparing the individual models together, it is found that the overall weakest wood/glue combination is Spruce Pine wood with PUR1 glue (3.1). Furthermore, the second weakest combination is Spruce Pine wood with MF glue (3.4). Additionally, the strongest combination is Douglas Fir wood with PUR1 glue (1.1). Both 3.1 and 3.4 will be tested at varying ply's, but 1.1

will also be tested, to maintain contrast between the strong combination and the weak combinations.

Table 4.5 Deflection Stiffness of Panel at Specified Temperatures

Model Number	Panel Deflection Stiffness at Specified Temperature (lbs/in.)					
	25°C	80°C	135°C	190°C	245°C	300°C
3.1.1	630.4	622.7	614.9	606.9	598.9	590.7
3.1.2	628.4	620.7	612.8	604.9	596.9	588.7
3.1.3	630.3	622.5	614.7	606.8	598.7	590.6
3.1.4	626.5	618.8	611.0	603.0	595.0	586.8
3.2.1	612.4	601.2	589.9	578.3	566.4	554.3
3.2.2	610.5	599.4	588.0	576.4	564.6	552.5
3.2.3	612.4	601.2	589.9	578.3	566.4	554.3
3.2.4	608.6	597.5	586.1	574.5	562.7	550.5
3.3.1	529.2	521.0	512.7	504.2	495.5	464.1
3.3.2	527.4	519.2	510.8	502.3	493.7	484.9
3.3.3	529.2	521.0	512.7	504.2	495.5	486.7
3.3.4	525.5	517.3	509.0	500.5	491.8	483.0

Table 4.6 Visual Categorization of Panel Deflection Stiffness Compared to Temperature

Model Number	Panel Deflection Stiffness at Specified Temperature (lbs/in.)					
	25°C	80°C	135°C	190°C	245°C	300°C
3.1.1	630.4	622.7	614.9	606.9	598.9	590.7
3.1.2	628.4	620.7	612.8	604.9	596.9	588.7
3.1.3	630.3	622.5	614.7	606.8	598.7	590.6
3.1.4	626.5	618.8	611.0	603.0	595.0	586.8
3.2.1	612.4	601.2	589.9	578.3	566.4	554.3
3.2.2	610.5	599.4	588.0	576.4	564.6	552.5
3.2.3	612.4	601.2	589.9	578.3	566.4	554.3
3.2.4	608.6	597.5	586.1	574.5	562.7	550.5
3.3.1	529.2	521.0	512.7	504.2	495.5	464.1
3.3.2	527.4	519.2	510.8	502.3	493.7	484.9
3.3.3	529.2	521.0	512.7	504.2	495.5	486.7
3.3.4	525.5	517.3	509.0	500.5	491.8	483.0

4.4.1 Effects with Varying Plys

Having determined the weakest and strongest combinations of wood and glue, the next step of testing is to see how changing the amount of ply's in the CLT impacts the results. In order to fully test this, the following testing schedule was determined, where the model naming convention is the same however, the first number now represents the number of ply's being tested. The combinations are seen in Table 4.7:

Table 4.7 Second Stage CLT Testing Matrix

	25°C	80°C	135°C	190°C	245°C	300°C
5 Ply	5.1.1.025	5.1.1.080	5.1.1.135	5.1.1.190	5.1.1.245	5.1.1.300
	5.3.1.025	5.3.1.080	5.3.1.135	5.3.1.190	5.3.1.245	5.3.1.300
	5.3.4.025	5.3.4.080	5.3.4.135	5.3.4.190	5.3.4.245	5.3.4.300
7 Ply	7.1.1.025	7.1.1.080	7.1.1.135	7.1.1.190	7.1.1.245	7.1.1.300
	7.3.1.025	7.3.1.080	7.3.1.135	7.3.1.190	7.3.1.245	7.3.1.300
	7.3.4.025	7.3.4.080	7.3.4.135	7.3.4.190	7.3.4.245	7.3.4.300

The increment of the temperature step is maintained at this stage of testing, as it is a reasonable assumption that the linear trend in data will continue. However, as the number of ply's increases, so does the number of nodes and elements that the analysis has to handle. This significantly slows down this portion of the testing, hence not all of the wood and glue combinations were used to test the effects of varying ply's. Thus, the two weakest combinations (3.1 and 3.4) are chosen to test with an increased number of ply's. Additionally, the strongest combination (1.1) is tested alongside the others as a reference point for the data. These are run following the above testing schedule, with the only other change being an increased point load of 1000 lbs. The load is increased due to the presumed increase in strength/stiffness by having

more ply's. The test results are presented in the following figures and tables, starting with the displacements in Figure 4.2.

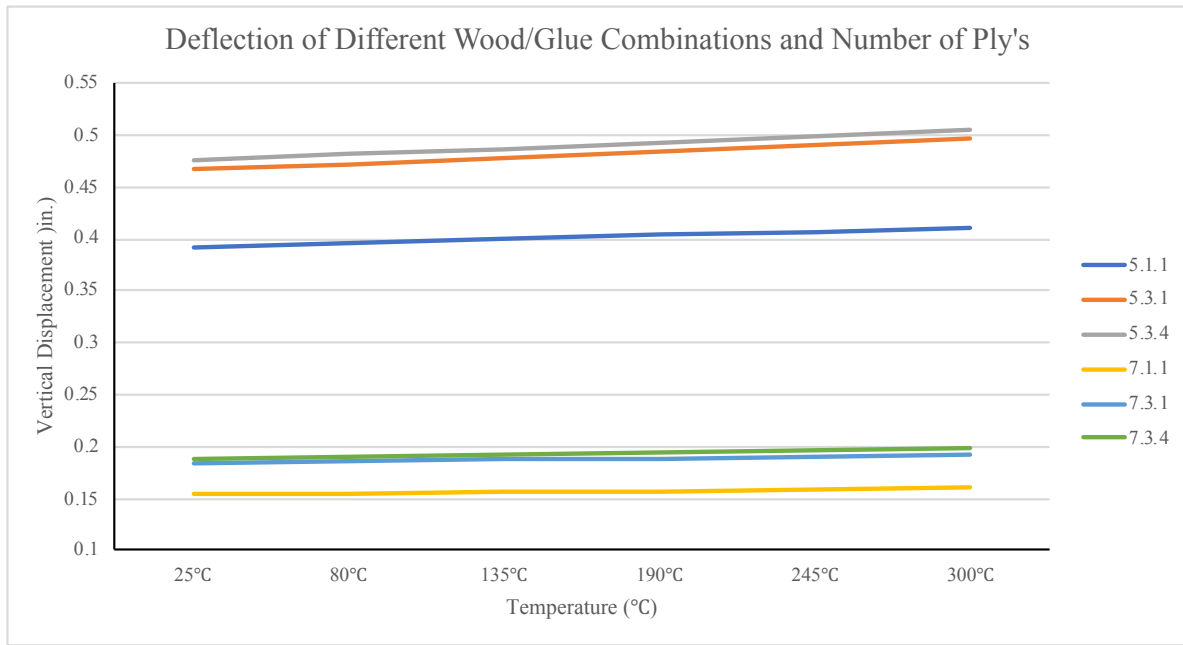


Figure 4.2 Panel Deflection of 5 and 7 Ply Panels

The results from the initial displacements are consistent with the results seen in the 3 ply models. The over-all trend is a linear increase in the amount of deflection each combination exhibits over the temperature range. Similarly, the pattern of the models remains the same, i.e. the two weakest combinations show a higher amount of deflection when compared to the strongest combination. This is displayed in Figure 4.2 by the significant gap in deflection between the weak and strong combinations, however the number of ply's still remain clustered to each other leaving a distinct gap between ply counts. Glue types PUR1 and MF remain close in value however, still maintain a noticeable difference in deflection as well. Furthermore, it can be noted that the slope of the linear regression significantly decreases as the number of ply's is

increased. The next comparison to be made is the limit stress load and material, as well as the reduction in limit stress load, as seen in Table 4.8 and Table 4.9 respectively.

Table 4.8 Limit Stress Target Load and Material of Multi-Ply Combinations

Model Number	Limit Stress Target Load at Specified Temperature (lbs) and Limiting Material											
	25°C		80°C		135°C		190°C		245°C		300°C	
5.1.1	1058.2	Wood	1052.6	Wood	1046.9	Wood	1041.0	Wood	1035.1	Wood	1029.1	Wood
5.3.1	745.3	Wood	740.2	Wood	735.0	Wood	729.8	Wood	724.4	Wood	718.9	Wood
5.3.4	730.3	Wood	725.3	Wood	720.2	Wood	715.1	Wood	709.8	Wood	704.3	Wood
7.1.1	1920.7	Wood	1914.6	Wood	1908.5	Wood	1902.3	Wood	1896.1	Wood	1888.7	Wood
7.3.1	1365.0	Wood	1357.2	Wood	1349.3	Wood	1341.2	Wood	1333.1	Wood	1324.8	Wood
7.3.4	1311.3	Wood	1306.2	Wood	1301.0	Wood	1295.6	Wood	1290.1	Wood	1284.6	Wood

Similar to the results seen in only the 3-ply models, wood remains the consistent limit material for the models. Out of the wood types, the Douglas Fir models still exhibit a higher strength than the Spruce Pine models.

Table 4.9 Reduction in Limit Stress Target Loads for Multi-Ply Combinations

Model Number	Percent Reduction in Stress Limit Target Load					
	25°C	80°C	135°C	190°C	245°C	300°C
5.1.1	0.00	-0.53	-1.07	-1.63	-2.18	-2.75
5.3.1	0.00	-0.68	-1.38	-2.08	-2.80	-3.54
5.3.4	0.00	-0.68	-1.38	-2.08	-2.80	-3.56
7.1.1	0.00	-0.32	-0.64	-0.96	-1.28	-1.67
7.3.1	0.00	-0.57	-1.15	-1.74	-2.34	-2.95
7.3.4	0.00	-0.39	-0.79	-1.20	-1.62	-2.04

The results from this portion of the study are consistent with the overall linear trend again. The maximum load for the 5 and 7 ply models all decreased linearly as the temperature increased, as seen in Table 4.9. However, the significant change in the 5 and 7 ply models,

compared to the 3 ply models, is the higher values for the stress limit target load. This pattern is again consistent against beam theory, as a thicker cross section lends to higher stiffness and higher strength. The changes in the deflection can be seen in the following table.

Table 4.10 Panel Stiffness Trends for Varying Wood/Glue Combinations

Model Number	Panel Deflection Stiffness at Specified Temperature (lbs/in.)					
	25°C	80°C	135°C	190°C	245°C	300°C
5.1.1	2551.2	2527.5	2503.7	2479.7	2455.4	2430.9
5.3.1	2141.6	2116.5	2091.2	2065.6	2039.7	2013.5
5.3.4	2104.0	2079.0	2053.4	2028.1	2002.3	1976.1
7.1.1	6495.5	6447.9	6399.8	6351.5	6302.9	6253.9
7.3.1	5448.0	5397.6	5346.8	5295.5	5243.8	5191.6
7.3.4	5318.9	5268.6	5217.8	5166.6	5115.0	5062.8

The above table lists the over-all panel stiffness of the different models when compared to temperature. The trend is a linear decrease in a model’s stiffness as the temperature increases. This maintains the consistency for the material properties of the beam as well as the trend in the stress limit load. This pattern is important in that it allows for consistent prediction in the material behavior of the different combinations.

4.4.2 comparisson between 3, 5, and 7 ply CLT

To form a better understanding of how the material properties, change with the effect of temperature, the linear regression was calculated for stiffness, maximum load, and displacement. These values are determined by finding the slope over the range of temperature, which are then converted into the slope per 55°C step size. This is done to represent the data in the context of this study. This is summarized in Table 4.11 (page 54).

Table 4.11 Comparison of Trends Between Varying Ply Count

Model Number	Douglas Fir and PUR1			Spruce Pine and PUR1			Spruce Pine and MF		
	3.1.1	5.1.1	7.1.1	3.3.1	5.3.1	7.3.1	3.3.4	5.3.4	7.3.4
Stiffness (lbs/in)/55 °C	-7.947	-24.048	-48.333	-11.730	-25.615	-48.333	-8.499	-25.574	-51.213
Target Load lbs/55°C	-3.074	-5.826	-6.334	-2.822	-5.275	-8.040	-2.777	-5.186	-5.349
Deflection in/55°C	0.011	0.004	0.001	0.024	0.006	0.002	0.017	0.006	0.002

A few interesting observations can be drawn from Table 4.9 above. First and foremost is the consistency in the overall trend of the study. The Douglas Fir and PUR1 models all maintained the highest strength/stiffness, while the Spruce Pine and PUR1 models took second to weakest, and the Spruce Pine and MF models were the lowest. Secondly, the displacement exhibited by each model decreases as the number of ply's are increased, which was expected. It is important to note that the 5 and 7 ply models had an increased point load applied, meaning that their displacement values cannot be directly compared to the 3-ply case. They are included in order to show the trend. However, the most significant trend that can be observed is the increase in regression as the ply's were increased for the stiffness and max load. Looking at the Douglas Fir and PUR1 model's specifically, the stiffness sees the biggest change per 55°C increment. With 3 ply's the stiffness is lowered by roughly 8 lbs/in every time the temperature is increased 55°C. For the 5-ply case, this value is tripled, being rough 24 lbs/in, which is then doubled again for the 7-ply case being roughly 48 lbs/in. The significance of this trend meaning that while models with a higher ply counts show lower deflections, they also exhibit a quicker decay in strength with increased ply numbers. This trend is also seen in the maximum load, albeit at a small scale. This observation seemingly contradicts the expectation that using higher ply counts would reduce the amount of decay in strength and stiffness. A possible cause for this might be

that the fire directly impacts the extreme fibers of CLT, which play a more significant role at thicker panel depths. This meaning that as the extreme fibers move further away from the panel's axis of rotation, they absorb more load than the rest of the panel, thus as they weaken, more of the load has to be transferred into the intermediate layers of perpendicular wood. This impacts the stiffness and strength of the panel due to the fact that the layers of perpendicular wood have a much lower ability to resist tensile force due to their configuration. This can be seen by comparing contours of the internal tension stress of a model over the different ply counts, as illustrated in the following set of figures. All of these figures are plotted for the Douglas Fir and PUR1 combination (1.1).

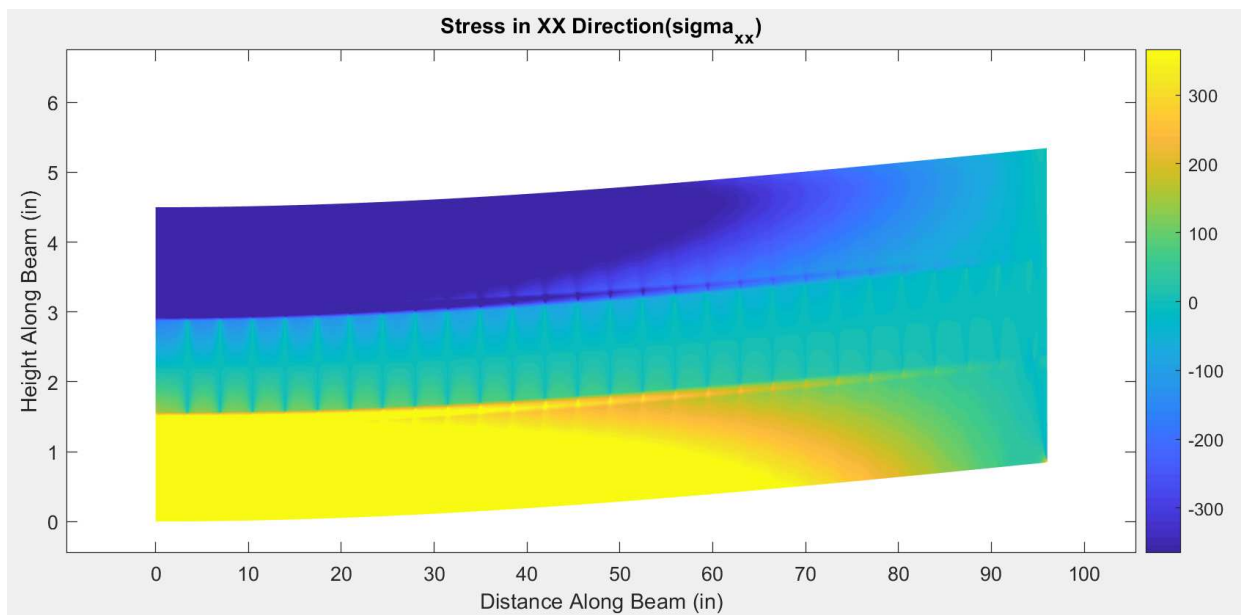


Figure 4.3 Internal Stress in X Direction for 300°C 3-Ply Model

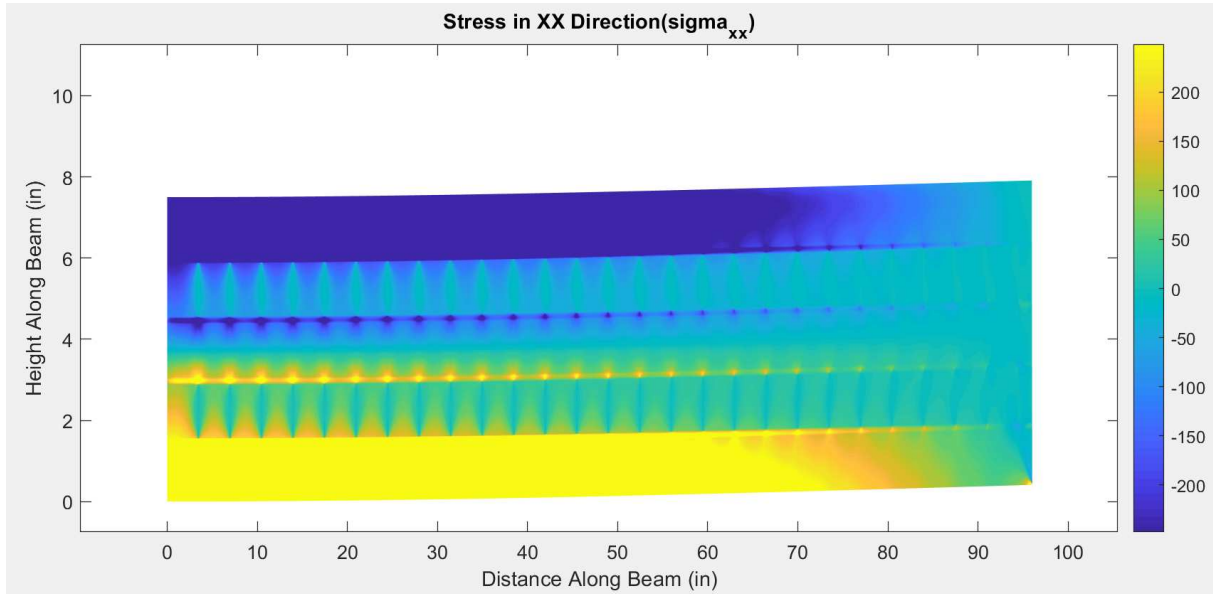


Figure 4.4 Internal Stress in X Direction for 300°C 5-Ply Model

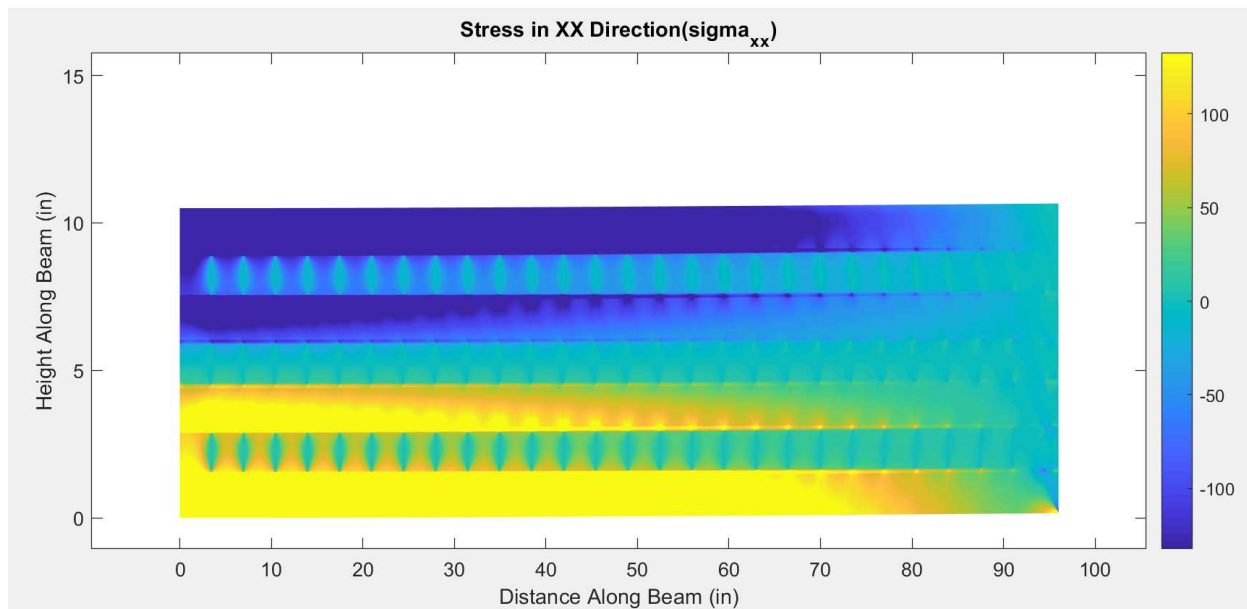


Figure 4.5 Internal Stress in X Direction for 300°C 7-Ply Model

These plots are excellent at visualizing what is discussed earlier. As the number of ply's increase, the apparent amount of shear stress in the lower elements of the panel increases. This

is slightly more difficult to see in Figure 4.3 (page 55) for the 3-ply case, but the tensile stress (visualized by the yellow) portion on the bottom of the panel is slightly larger than the compression stress (visualized by the blue) at the top of the panel. As expected, the perpendicular inner layers remain close to zero due to their lowered strength. Looking at Figure 4.4 (figure 56) for the 5-ply case, the amount of tensile stress in the bottom of the panel is slightly easier to identify. Similarly, the layers of perpendicular wood remain close to zero in their stress, while the compression side of the panel has a slightly smaller area than the tension. And finally, this pattern is accentuated more in Figure 4.5 (page 56) for the 7-ply case. The tensile stress on the bottom of the panel is again more apparent than the compression stress at the top of the panel. This overall confirms the reasoning that increased layers are impacted more due to the application of elevated temperatures.

Another interesting trend that is noticed here is in the behavior of the middle layer, made of wood in its strong direction. The majority of this layer has little to no stress impacting it apart from small regions of concentrated stress located at the edge glue interface locations of the perpendicular wood layers. This pattern is likely due to the rotation of the inner layers as the panel deflects. The pattern is most apparent in Figure 4.4 (page 56) for the 5-ply case, however both Figure 4.3 (page 55) and Figure 4.5 (page 56) show this pattern for the 3-ply and 7-ply case respectively. This pattern is to be expected from the model, however it is more apparent in plots of the shear stress and strain, as shown in Figures 4.6 (page 58) and Figures 4.7 (page 59) below for the 7-ply case. It is significant that this pattern is seen in the x direction.

The trend for these plots is almost reversed from the trend in the x stress figures. With stress in the x direction, the internal stress concentrations were seen in the strong wood direction, while in Figures 4.6 (page 58) and 4.7 (page 59), this trend is flipped where the concentrations

are seen in the perpendicular wood elements themselves. However, the bigger stress concentrations still occur in the outermost layers of the perpendicular wood. The most likely cause of these is due to these wood elements trying to rotate as the panel bends. These elements are unrestrained at two sides, allowing for the rotation and thus the resulting in the concentrations as seen above.

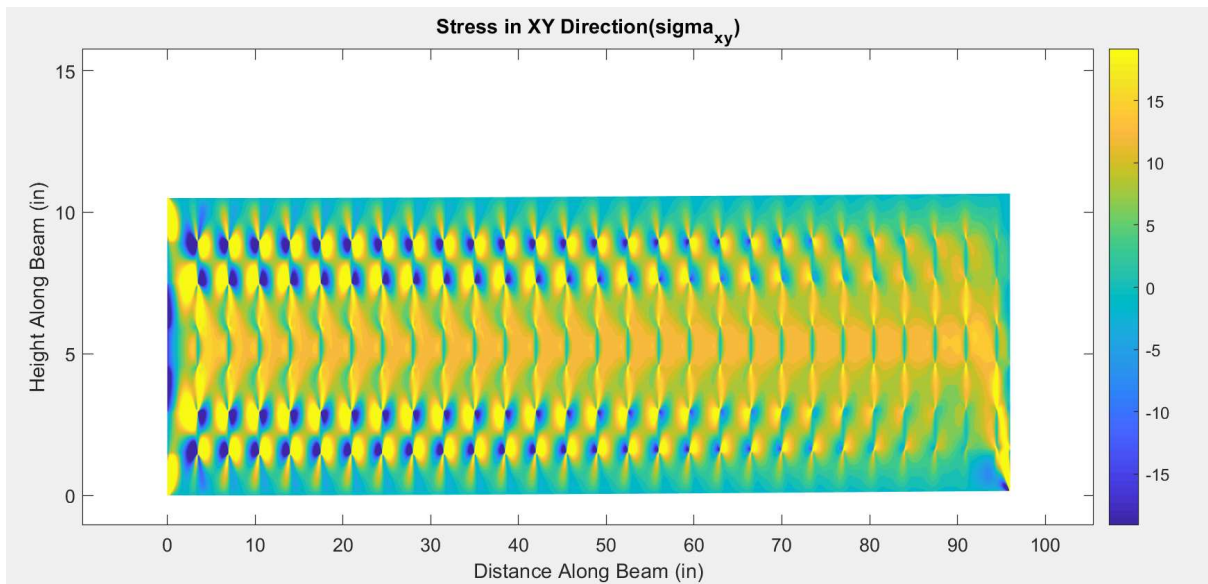


Figure 4.6 Shear Stress for 7-Ply Model at 300°C Temperature

Overall, there are significant differences in the amount of ply's used in a one-way CLT slab panel. While the overall panel will only reach failure in its outermost fibers, there are still a significant amount of inner stresses and strains that contribute to the panel's performance with elevated temperatures.

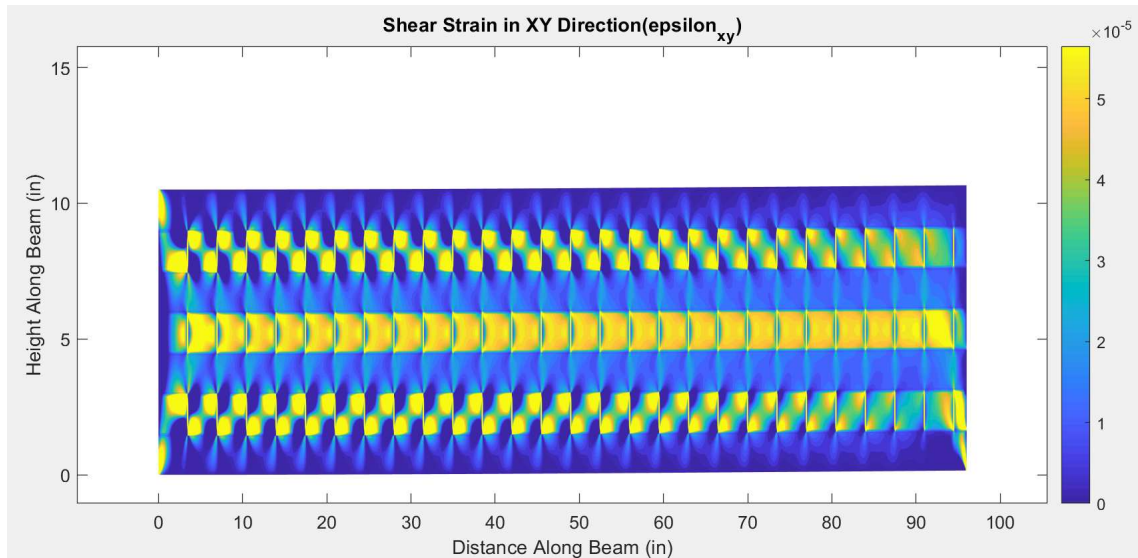


Figure 4.7 Shear Strain for 7-Ply Model at 300°C Temperature

4.5 Tested temperature profile compared to potential temperature profile

Overall, the tests did reveal information about the change in material properties, however the ultimate change was rather negligible. This is due to the very limited amount of material that the fire impacts on the panel. Referring back to Figure 3.1 of the panel's temperature profile, the effects of the fire really only impact the wood for just over 1 inch. The rest of the panel remains unaffected by the fire applied below, which is significant given that the first layer of glue is 1.5 inches into the panel. The obvious conclusion from this is that wood acts as a much better insulator than originally expected. However, the test data the temperature profile is based on is only from a singular trial on a panel. The experimental data realistically can't be considered the only temperature profile to exist, any number of factors could change the way that temperature propagates through a panel. For example, variances in moisture content could impact the profile, or even different wood species could impact the profile. In order to understand how changes to the wood as well as glue impact the overall behavior, a temperature profile impacting more than

1 inch of wood is developed. The assumption that the wood has an exponential regression will remain constant, however the exponential value will be altered in order to increase the impacted area. The new linear regression to be considered is plotted in Figure 4.8 below, alongside the experimental temperature profile for comparison.

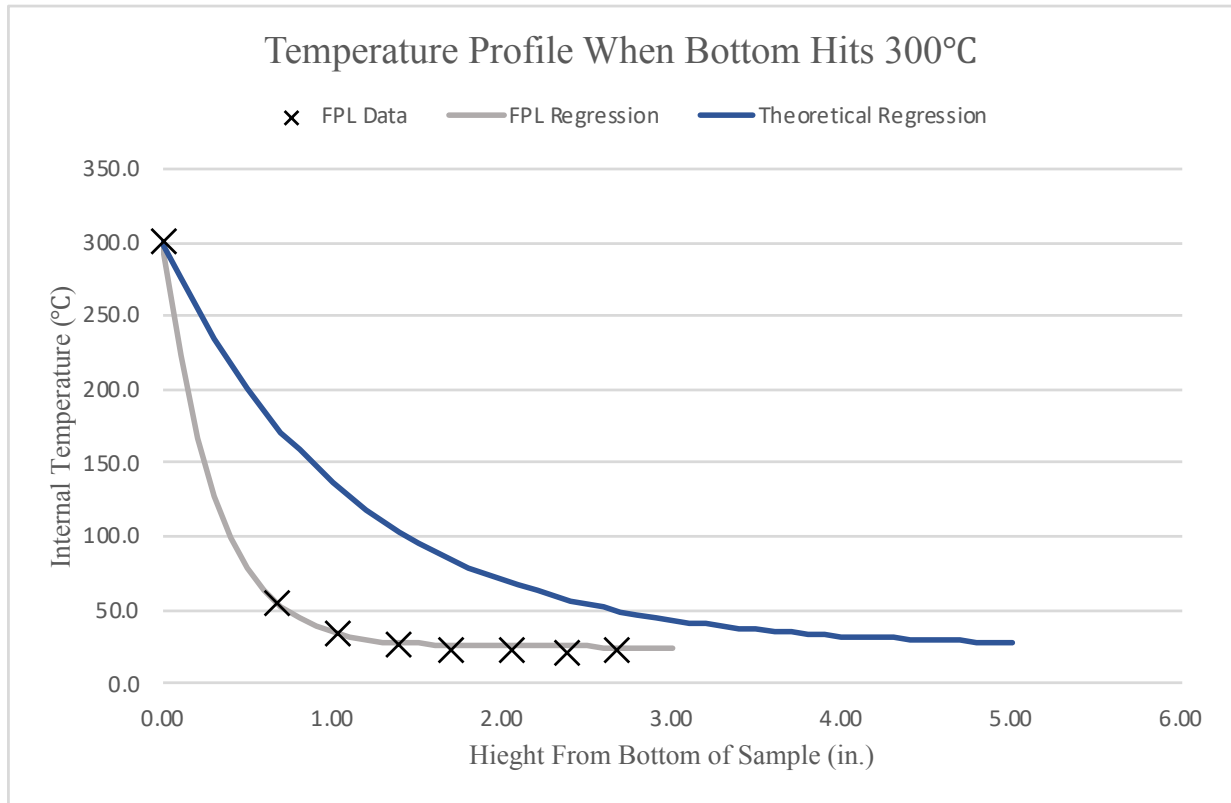


Figure 4.8 Theoretical Temperature Profile

The test results obtained from FPL are illustrated by the X's while their trendline is illustrated by the gray line. The dark blue line is the curve to be tested where the effect of the temperature returns to normal roughly 4 inches into the panel. The basis for this theoretical curve is to increase the affected area while maintaining the idea that the temperature still has not fully propagated through the material. The general method of developing this curve was simply

changing the y multiplier in the original regression curve. Realistically, if temperature propagates the same in all wood species, this would be the only factor that affects the rate, thus it was adjusted until the desired curved was achieved. In this case, the value changed from -3.3 for the experimental data to -0.9 for the theoretical curve. The new equation is listed below:

$$T = 25 + (T_i - 25)e^{-0.9y} \quad (4.1)$$

Based on this theoretical temperature profile, the extent of the impacted are is verified in Figure 4.9 (page 62). The fire impact plot is generated in the same way as Figure 4.1 (page 44) from before in order to visually describe the impact on the panel.

The overall impact of the theoretical temperature profile is much more significant, as seen in Figure 4.9 (page 62). The extent of this impact goes to around 4 inches of height in the panel. While it is difficult to tell from the contour, the shading of the lowered modulus of elasticity values does in fact extend to the expected height. Having verified the application of the theoretical profile, the desired wood glue combinations are selected in order to run the analyses. In this case, only three combinations were tested. All wood species were tested to see their varying results, while only PUR1 was tested with these woods, considering it has the highest glue strength from the previous tests. Thus, a new testing matrix is developed and displayed in Table 4.12 (page 63), following the same naming conventions as previous models.

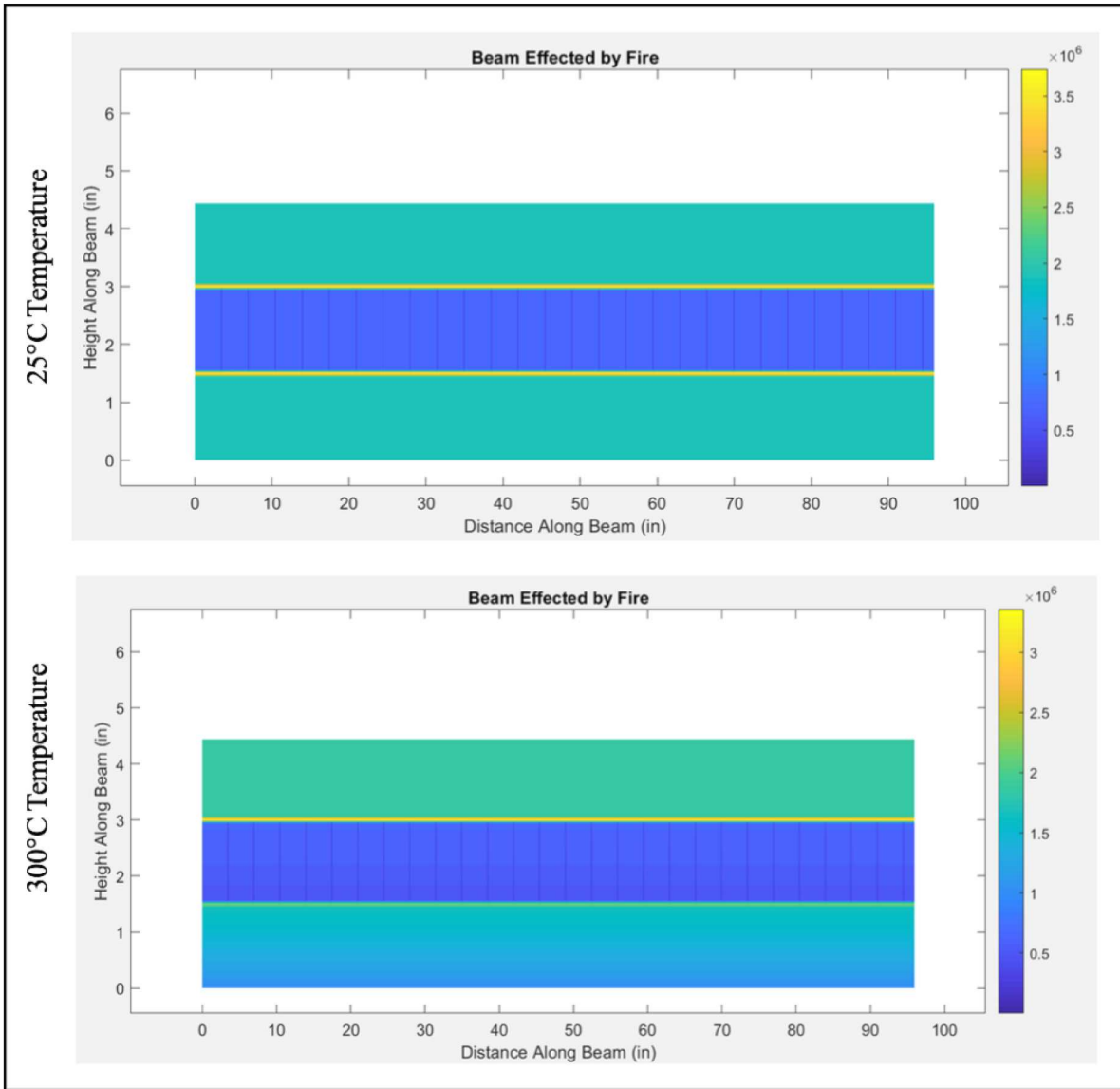


Figure 4.9 Extent of Fire Impact Using Theoretical Temperature Profile

As stated, the three different combinations to be tested are 1.1, 2.1, and 3.1. They will be tested over the same temperature range as well incrementing the temperature by 55°C steps. To be consistent with the previous tests, the 3 ply models will be tested with a 500 lb load, while the 5 and 7 ply models will be tested with a 1000 lb load. The test data for these new panel models

are presented below, beginning with the failure modes considering the theoretical temperature profile, show in Table 4.13.

Table 4.12 Testing Matrix for Theoretical Temperature Profile

	25°C	80°C	135°C	190°C	245°C	300°C
3 Ply	T.3.1.1.025	T.3.1.1.080	T.3.1.1.135	T.3.1.1.190	T.3.1.1.245	T.3.1.1.300
	T.3.2.1.025	T.3.2.1.080	T.3.2.1.135	T.3.2.1.190	T.3.2.1.245	T.3.2.1.300
	T.3.3.4.025	T.3.3.4.080	T.3.3.4.135	T.3.3.4.190	T.3.3.4.245	T.3.3.4.300
5 Ply	T.5.1.1.025	T.5.1.1.080	T.5.1.1.135	T.5.1.1.190	T.5.1.1.245	T.5.1.1.300
	T.5.3.1.025	T.5.3.1.080	T.5.3.1.135	T.5.3.1.190	T.5.3.1.245	T.5.3.1.300
	T.5.3.4.025	T.5.3.4.080	T.5.3.4.135	T.5.3.4.190	T.5.3.4.245	T.5.3.4.300
7 Ply	T.7.1.1.025	T.7.1.1.080	T.7.1.1.135	T.7.1.1.190	T.7.1.1.245	T.7.1.1.300
	T.7.3.1.025	T.7.3.1.080	T.7.3.1.135	T.7.3.1.190	T.7.3.1.245	T.7.3.1.300
	T.7.3.4.025	T.7.3.4.080	T.7.3.4.135	T.7.3.4.190	T.7.3.4.245	T.7.3.4.300

Table 4.13 Limiting Stress and Material for Theoretical Temperature Profile

Model Number	Limit Stress Target Load at Specified Temperature (lbs) and Limiting Material											
	25°C		80°C		135°C		190°C		245°C		300°C	
T.3.1.1	430.5	Wood	421.3	Wood	411.7	Wood	401.5	Wood	390.8	Wood	379.5	Wood
T.3.2.1	708.1	Wood	686.5	Wood	663.2	Wood	637.9	Wood	610.0	Wood	578.7	Wood
T.3.3.1	302.3	Wood	293.8	Wood	284.8	Wood	275.1	Wood	264.8	Wood	253.5	Wood
T.5.1.1	1058.2	Wood	1041.1	Wood	1022.9	Wood	1003.6	Wood	982.9	Wood	960.8	Wood
T.5.2.1	1734.9	Wood	1693.2	Wood	1647.5	Wood	1597.2	Wood	1541.5	Wood	1479.2	Wood
T.5.3.1	745.3	Wood	729.7	Wood	712.9	Wood	694.8	Wood	675.0	Wood	653.4	Wood
T.7.1.1	1920.7	Wood	1902.1	Wood	1873.3	Wood	1841.1	Wood	1807.1	Wood	1771.3	Wood
T.7.2.1	3159.7	Wood	3088.7	Wood	3012.3	Wood	2929.8	Wood	2840.6	Wood	2743.4	Wood
T.7.3.1	1365.0	Wood	1338.5	Wood	1310.3	Wood	1280.3	Wood	1248.2	Wood	1231.9	Wood

The general trend of wood being the material to reach its limiting stress first is again emphasized in the results of the theoretical temperature profile. This trend is consistent with the mechanics of the panel. The middle of a member in bending is where the highest shear occurs, and, given the nature of both the theoretical and experimental temperature profiles in this study, the middle of the panels see a very low change in temperature. It can be concluded from this the,

that models using an exponential temperature profile will only see limiting stresses occurring in the wood. Additionally, these models will also only see a linear reduction in their limit stress load, which is seen in the experimental profile models, as well as the results of the theoretical profile models in Table 4.14 below.

Table 4.14 Reduction of Limit Stress Target Load Under Theoretical Temperature Profile

Model Number	Percent Reduction in Limit Stress Target Load					
	25°C	80°C	135°C	190°C	245°C	300°C
T.3.1.1	0.00	-2.14	-4.38	-6.75	-9.23	-11.86
T.3.2.1	0.00	-3.05	-6.34	-9.91	-13.85	-18.27
T.3.3.1	0.00	-2.83	-5.80	-9.01	-12.42	-16.16
T.5.1.1	0.00	-1.62	-3.34	-5.16	-7.12	-9.21
T.5.2.1	0.00	-2.40	-5.04	-7.94	-11.15	-14.74
T.5.3.1	0.00	-2.09	-4.35	-6.78	-9.43	-12.33
T.7.1.1	0.00	-0.97	-2.47	-4.14	-5.91	-7.78
T.7.2.1	0.00	-2.25	-4.66	-7.28	-10.10	-13.18
T.7.3.1	0.00	-1.94	-4.01	-6.21	-8.56	-9.75

As discussed based on Table 4.13 (page 63) above, the results seen in Table 4.14 are consistent with the failure modes of the panels. A trend that is consistent despite using a theoretical temperature profile is amount the maximum load changes over the given range. The southern pine models all show the biggest change in max loading despite changes to the amount of ply's. Similarly, the amount that the maximum load changes by increases as the ply count increases. This again goes against the expectation that increasing the thickness of the panel would decrease the amount of overall change. This trend is also seen in the panel's stiffness vs temperature and layers as seen in Table 4.15 (page 65).

Table 4.15 Deflection Stiffness of Panel Models Under Theoretical Temperature Profile

Model Number	Panel Deflection Stiffness at Specified Temperature (lbs/in.)					
	25°C	80°C	135°C	190°C	245°C	300°C
T.3.1.1	630.3	608.2	585.3	561.2	536.1	509.6
T.3.2.1	612.4	580.6	546.7	510.4	471.3	428.8
T.3.3.1	529.2	505.7	480.9	454.7	426.7	396.8
T.5.1.1	2551.2	2486.8	2393.9	2310.9	2224.6	2135.0
T.5.2.1	2457.2	2379.6	2231.3	2108.7	1978.9	1840.8
T.5.3.1	2141.6	2059.5	1973.7	1883.7	1789.2	1689.7
T.7.1.1	6495.5	6325.4	6150.2	5969.8	5783.9	5592.2
T.7.2.1	6219.6	5979.5	5728.9	5467.1	5193.1	4905.9
T.7.3.1	5448.0	5267.9	5081.1	4887.1	4685.6	4475.9

Again, the results presented above follow the trend of the study. Douglas Fir models show the largest stiffness overall, compared to Southern Pine models with the second highest stiffness, and Spruce Pine models showing the weakest stiffness. Similarly, the rate of decay follows the odd pattern of increasing with thickness. For Douglas Fir models, the 3-Ply stiffness changes by roughly 120 lbs/in, while the 5-ply stiffness changed by 220 lbs/in, and the 5-ply stiffness changed by roughly 900 lbs/in. The change in these properties is quite interesting but is likely due to the cause discussed in section 4.4.2 above. The highest stress in the wood occurs in the most extreme fibers, and it is likely that as these fibers weaken when farther away from the axis of rotation, they play a larger role on the panel's properties. To see if the extent of this effect is changed with the theoretical temperature profile, the stresses in the x direction are contoured for the Douglas Fir and PUR1 combination (1.1) for each ply count.

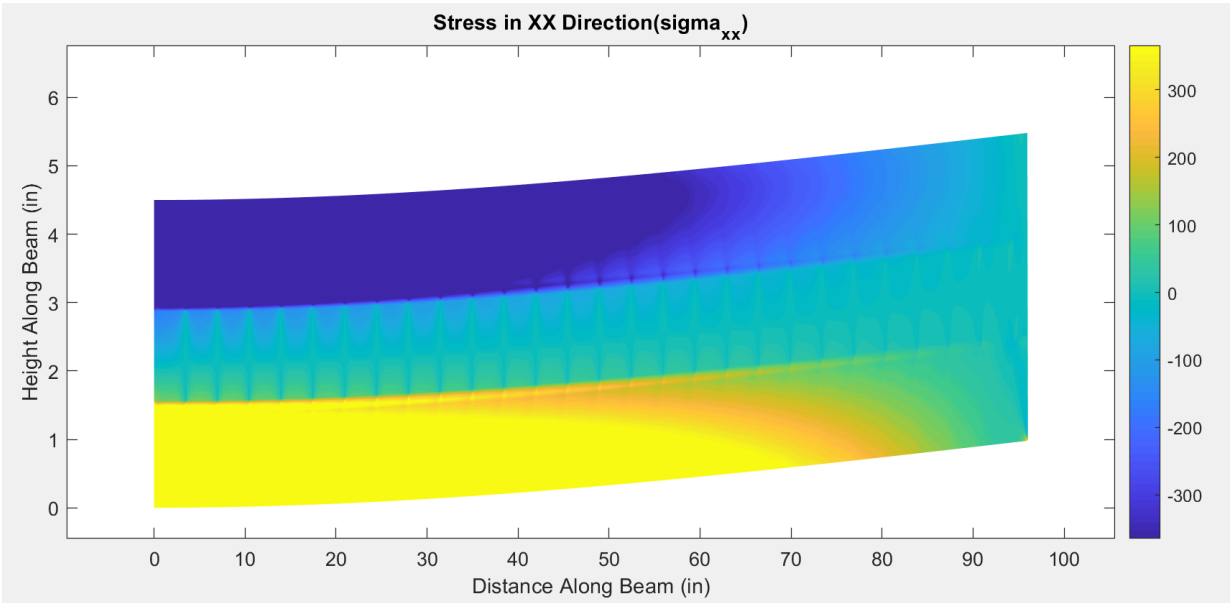


Figure 4.10 Internal Stress in X Direction for 300°C 3-Ply Model with Theoretical Profile

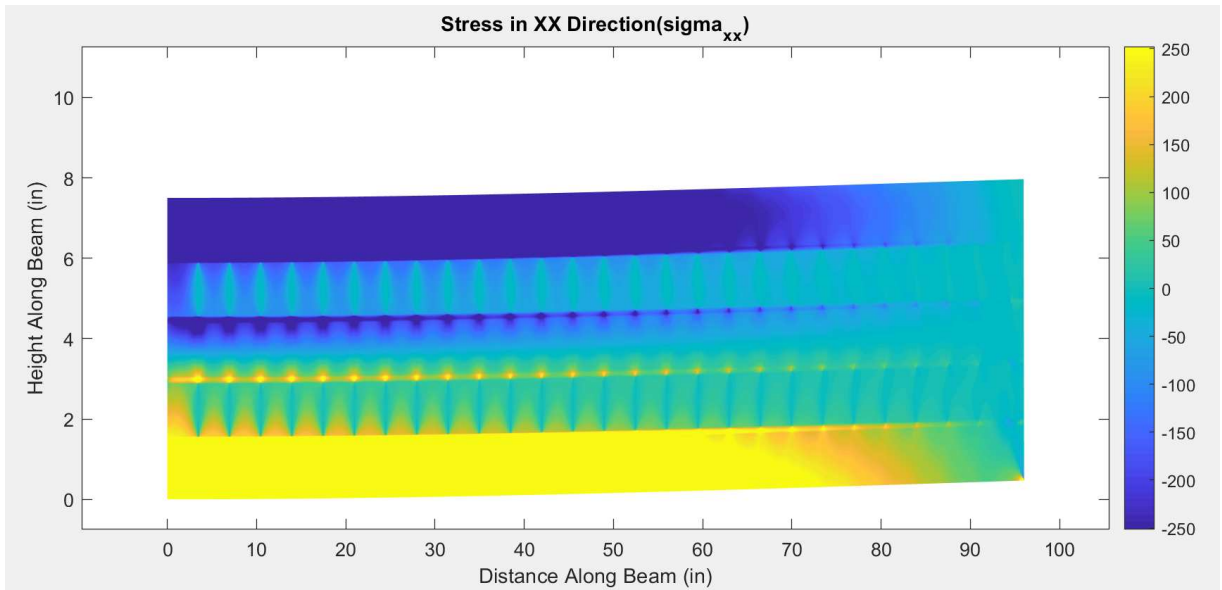


Figure 4.11 Internal Stress in X Direction for 300°C 5-Ply Model with Theoretical Profile

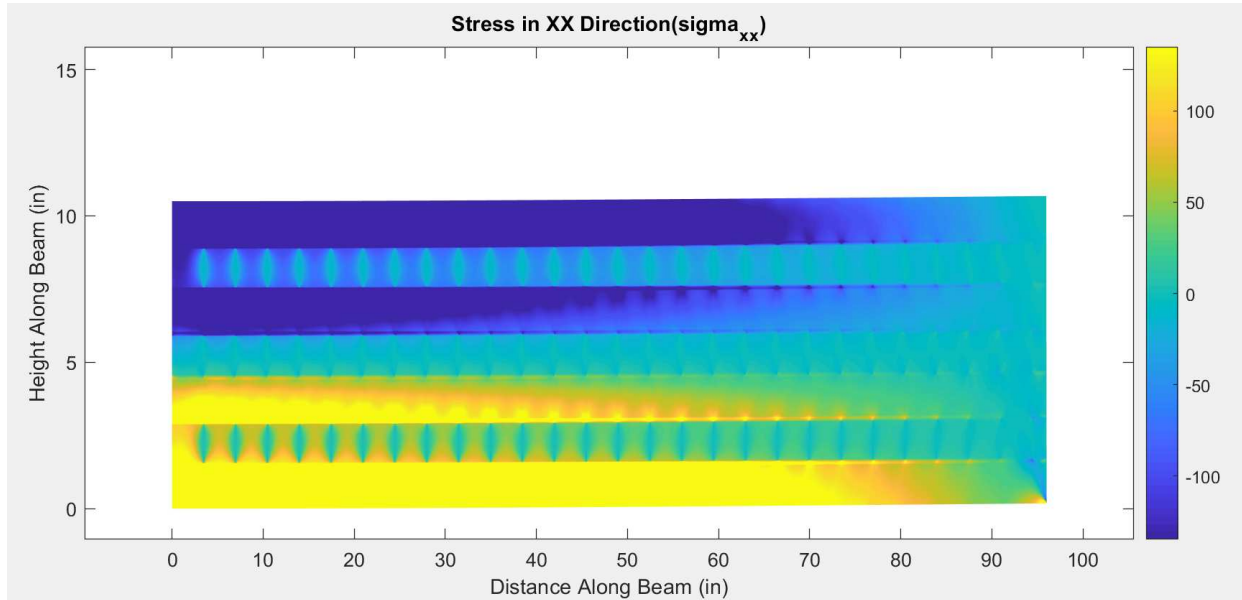


Figure 4.12 Internal Stress in X Direction for 300°C 7-Ply Model with Theoretical Profile

The overall trend in these plots is much more apparent than the trend of seen in the experimental temperature profile. Figure 4.10 (page 66) shows a much more visible difference in tensile and compressive stress for the 3-ply case. This is seen again in Figure 4.11 (page 66) for 5-ply and then again in Figure 4.12 for 7-ply's. Additionally, the stress concentrations around the perpendicular wood layers are also seen again.

The biggest change in using the theoretical temperature profile is in the deflection, strength, and stiffness of the different models. Apart from that, there are no significant changes in the panel behavior, thus it is reasonable to say that the performance of CLT at elevated temperatures will respond in a predictable pattern, based on the tested parameters of this study.

CHAPTER FIVE: CONCLUSION

The goal of this study was to determine the structural performance of CLT at elevated temperatures in order to better understand how to implement CLT as a one-way slab in building design. The findings from this study do lend more information to this topic and quite a few conclusions are drawn. The main conclusions were related to the effect of wood and glue combinations on panel stiffness and strength, and the variation of the structural properties with different temperature profiles.

In terms of the structural performance of CLT at elevated temperatures, the results are consistent with what is expected. Fire does change the strength and stiffness of a given CLT panel, however, the amount of change is not very significant. For a 16 foot one-way slab, the biggest difference in deflection was roughly only 10% of the deflection at room temperature. Although this study does not directly address strength at the failure of the panels, it indirectly identified the load level (allowable load) at which the wood or glue components in a panel will reach their allowable stress level when adjusted by temperature. It is found that wood consistently remains the material that reaches the limit state first. This is due to the higher shear forces being located at the neutral axis locations of the slab where temperature is not elevated a significant amount. The general trend in the allowable load level is less than a 5% reduction from 25°C to 300°C, when considering the experimentally developed temperature profile. When considering the theoretical temperature profile (where the insulation of the wood temperature is not as effective), the reduction in load level changes to roughly 11% in the given temperature range. This change is consistent throughout the models and combinations. This effect becomes even less pronounced as the number of CLT ply's was increased. The insensitive nature of CLT

to elevated temperatures is mainly due to the insulating properties of wood. Only a very small portion of the panel sees any impact from the temperature (about 1-2 inches on the bottom of the panel), thus the panel roughly maintains its structural performance in all other locations. In terms of the optimal combinations of wood and glue, it was found that Douglas Fir and PUR1 performed the best out of the type of materials covered in this study. Both Douglas Fir and PUR1 out-performed the other sample types regardless of ply count or applied temperature profile. Thus it can be concluded that CLT manufacturing with these two materials will yield the slightly better results as a bending member in high temperature scenarios.

The limitation of this study is that the results are all numerical, thus additional full-scale panel testing under high temperature will be needed to further validate the simulation results. The study also stopped at the temperature level where the exposed wood layer started to char. In traditional analysis, the wood material reaching temperatures above 300°C will be discarded as char in design. Thus, results from this study are more applicable to wood structures which are protected from fire by non-combustible layers (such as gypsum board) while reaching high temperatures. Finally, the scope of this study was limited to the glue types and the wood species that were tested.

REFERENCES

- [1] FPInnovations, "CLT Handbook: Cross Laminated Timber," Special Publication SP-529E ed: FPInnovations
Co-Published by U.S. Department of Agriculture
Forest Service Products Laboratory
Binational Softwood Lumber Council, 2013.
- [2] Y. Kim, J. F. Davalos, and E. J. Barbero, "Composite Beam Element with Layerwise Plane Sections," vol. 120 ed. ASCE: Journal of Mechanical Engineering, 1994, pp. 1160-1166.
- [3] P. Foraboschi, "Analytical Solution of Two-Layer Beam Taking into Account Nonlinear Interlayer Slip," vol. 135 ed. Journal of Mechanical Engineering: ASCE, 2009, pp. 1129-1146
- [4] S. Schanbi, M. Saje, G. Turk, and I. Planinc, "Analytical Solution of Two-Layer Beam Taking into account Interlayer Slip and Shear Deformation," vol. 133, ed. Journal of Structural Engineering: ASCE, 2007, pp. 886-894.
- [5] M. Klippel, C. Leyder, A. Frangi, and M. Fontana, "Fire Tests on Loaded Cross-Laminated Timber Wall and Floor Elements," ed. Fire Safety Science-Proceedings of the Eleventh International Symposium: International Association for Fire Safety Science, 2014 pp. 623-639.
- [6] A. Frangi, M. Fontana, M. Knobloch, and G. Bochicchio, "Fire Behavior of Cross-Laminated Solid Timber Panels," ed. Fire Safety Science-Proceeding of the Ninth International Symposium: International Association for Fire Safety Science, 2009, pp. 1279-1290.
- [7] S. Kineham, D. Thomson, A. Barlett, L. Bisby, and R. Hadded, "Structural Response of Fire-Exposed Cross-Laminated Timber Beams Under Sustained Loads," vol. 85, ed. Fire Safety Journal, 2016, pp. 23-34.
- [8] S. Zelinka *et al.*, "Small scale tests on the performance of adhesives used in cross laminated timber (CLT) under elevated temperatures," ed, 2018.
- [9] "OpenSees 3.0.3." University of California, Berkeley. opensees.berkeley.edu (accessed 2019).
- [10] A. W. Council, "2018 National Design Specification," ed. www.AWC.org, 2018.

[11] "Chapter 3: Properties of Wood and Structural Products," *USFS Timber Bridge Manual*.
www.dot.state.mn.us/bridge/pdf/insp/USFS-TimberBridgeManual/index.html 1992, ch. 3, p.
18.

[12] "MyCurveFit." MyAssays Ltd. *mycurvefit.com* (accessed 2019).